Háskólinn á Akureyri
University of Akureyri

Redirecting phosphorus from wastewater

Screening for phosphate accumulating bacteria from clam guts for potential wastewater remediation applications

Ísold Egla Guðjónsdóttir

Auðlindadeild
Heilbrigðis-, viðskipta- og raunvísindasvið
Háskólinn á Akureyri
2024

Redirecting phosphorus from wastewater

Screening for phosphate accumulating bacteria from clam guts for potential wastewater remediation applications

Ísold Egla Guðjónsdóttir

12 eininga lokaverkefni í Auðlindalíftækni
sem er hluti af
Baccalaureus Scientiarum-prófi í auðlindafræðum

Leiðsögukennarar
Eva María Ingvadóttir
Christina Goethel

Auðlindadeid
Heilbrigðis-, viðskipta- og raunvísindasvið
Háskólinn á Akureyri
Akureyri, apríl 2024

Titill: Redirecting phosphorus from wastewater: Screening for phosphate accumulating bacteria from clam guts for potential wastewater remediation applications
Stuttur titill: Redirecting phosphorus from wastewater
12 eininga bakkalárprófsverkefni sem er hluti af Baccalaureus Scientiarum-prófi í Auðlindafræðum.

Auðlindadeild
Heilbrigðis-, viðskipta- og raunvísindasvið
Háskólinn á Akureyri
Sólborg, Norðurslóð 2
600 Akureyri

Sími: 460 8000

Skráningarupplýsingar:
Ísold Egla Guðjónsdóttir, 2024, bakkalárprófsverkefni, Auðlindadeild, Heilbrigðis-, viðskipta- og raunvísindasvið, Háskólinn á Akureyri, 87 bls.

Prentun: Prentmet Oddi
Akureyri, apríl, 2024

Ágrip

Fosfór gegnir mikilvægu hlutverki í efnaskiptaferlum dreif- og heilkjarna frumna s.s. baktería, dýra og plantna. Þetta óendurnýjanlega steinefni er mikið notað í tilbúnum áburði í landbúnaði, en yfirvofandi skortur þess getur leitt til uppskerubrests og hungursneyðar á næstu árhundruðum ef ekkert verður að gert. Því er mikilvægt að loka hringrás fosfórs og koma í veg fyrir tap hans út í sjó, sem verður að hluta til vegna losunar skólps. Ísland er eftirbátur annarra vestrænna ríkja þegar kemur að skólphreinsun og sums staðar er óhreinsuðu skólpi enn veitt út í sjó. Áskoranir fráveitu á norðurslóðum felast m.a. í smæð byggðarlaga, köldu loftslagi og útþynntu skólpi. Markmið skólphreinsunar er að draga úr magni lífrænna og ólífrænna efna sem enda í viðtaka. Einn hluti hennar felst í að fjarlægja fosfór. Notkun sérhæfðra örvera (e. PAOs), sem hafa getu til að taka upp umframmagn fosfórs og mynda í leiðinni lífplast (e. PHA), í sérstöku "lifandi" kerfi (e. EBPR), hefur skilað bestum árangri.

Fimm óþekktir bakteríustofnar úr meltingarvegi kúfskeljar (*Arctica islandica*) úr Eyjafirði voru rannsakaðir m.t.t. fosfatupptöku og lífplastframleiðslu í tveimur gerðum gerviskólps (næringarríku og næringarsnauðu) við loftháðar aðstæður. Fosfatupptaka og lífplastframleiðsla mældist hjá öllum stofnum. Mesta framleiðsla lífplasts var 0.89 g/L PHA í næringarsnauðu gerviskólpi. Fosfatupptaka stofnanna var 17-30% í næringarsnauðu skólpi þegar upphafsstyrkur fosfats var 15.3 mg/L, sem svipar til hefðbundins upphafsstyrks og upptöku örvera í skólphreinsistöðvum. Í næringarríku skólpi var fosfórupptakan breytilegri en nálgaðist í sumum tilfellum 85%, sem nálgast skilvirkni EBPR. Þessar niðurstöður gefa tilefni til frekari rannsókna, því örverustofnar einangraðir hérlendis eru aðlagaðir staðbundnum aðstæðum og gætu komið að gagni við bæði hreinsun og virðisaukningu skólps í landinu.

Lykilorð: fosfór, fosfatupptaka, lífplast, skólphreinsun, fosfatupptakendur, kúfskel, Eyjafjörður

Abstract

Phosphorus serves an important role in the metabolism of both prokaryotes and eucaryotes, such as bacteria, animals and plants. This irreplaceable mineral is used in commercial fertilizer, but imminent shortage of the element could cause crop failure and worldwide famine within a few centuries if nothing is done. Therefore, recirculating phosphorus and preventing its loss to the sea, which can be partially attributed to wastewater effluent, is a pressing issue. Wastewater treatment in Iceland is underdeveloped compared to other Western countries and the wastewater from some towns is released untreated into the sea. The challenges of treating wastewater in Arctic regions are comprised of cold climate, small and distributed urban areas and diluted wastewater. The goal of wastewater treatment is to decrease the amount of organic and inorganic substances that end up in the receiving water body. One part of it is comprised of the removal of phosphorus. The utilization of specialized microbes (PAOs), which can accumulate phosphate in abundance and simultaneously synthesize bioplastics (PHA), in a specific type of "live" reactor (EBPR), has given the best results.

Herein, five unknown bacterial strains, isolated from the gut of the bivalve *Arctica islandica* sampled in Eyjafjörður, were examined with regard to aerobic phosphate accumulation and PHA production abilities in both nutrient-rich and nutrient-poor synthetic wastewaters (SWW). Measurements indicated phosphate accumulation and PHA production for all strains. The highest amount of produced PHA was 0.89 g/L. The strains' phosphate uptake was 17-30% in nutrient-poor SWW initially containing 15.3 mg phosphate/L, which resembles the conditions and efficiency of conventional wastewater treatment plants. The phosphate uptake varied more in the nutrient-rich SWW, with highest removal of 85%, which is close to the efficiency of EBPR. These results urge further research, as strains isolated in Eyjaförður are adapted to the local conditions and could benefit both the remediation and value-addition processes of wastewater in Iceland.

Keywords: phosphorus, phosphate accumulation, polyhydroxyalkanoates, wastewater treatment, phosphate accumulating organisms, bivalve, Eyjafjörður

Formáli

Frá því ég man eftir mér hef ég haft mikinn áhuga á náttúrunni og vísindum. Ég varð heilluð af líftækni þegar ég kynntist henni fyrst á Vísindavökunni í Laugardalshöll árið 2015. Þá ákvað ég að ég vildi verða líftæknifræðingur og nú er sá draumur loksins að verða að veruleika.

Mig langar að þakka leiðbeinanda mínum, Evu Maríu Ingvadóttur, kærlega fyrir frábæra leiðsögn í alla staði og fyrir að vilja til að taka þetta verkefni að sér og gefa sig alla í það, þrátt fyrir að efnið væri á vissan hátt utan við hennar svið. Einnig vil ég þakka henni fyrir að vera til staðar í gegnum allt BS námið og að koma þessari flugu í kollinn á mér á fyrsta ári. Christina Goethel, meðleiðbeinandi minn, á einnig skilið þakkir fyrir að eiga þátt í að þetta verkefni yrði að veruleika. Auk þess vil ég þakka Kolfinnu Ólafsdóttur og Kristni Pétri Kristinssyni fyrir hjálp og ráðgjöf við einangrun og mögnun erfðaefnis, sem og Jönu Lind Ellertsdóttur, Elínu Heiðu Hlinadóttur, Kötlu Maríu Kristjánsdóttur, Guðrúnu Jónu Jónmundsdóttur, Garðari Kára Garðarssyni, Þórdísi Sif Guðgeirsdóttur og síðast en ekki síst foreldrum mínum, Guðjóni Egilssyni og Rósu Hlín Óskarsdóttur, og ömmu minni Helenu Weihe, fyrir stuðning og félagsskap í gegnum árin.

Table of Contents

List of Figures

List of Tables

Abbreviations

ADP – Adenosine diphosphate
ATP – Adenosine triphosphate
BGA – Brilliant green agar
BOD – Biological oxygen demand
CLAAMs – Clam associated Arctic microbes
COD – Chemical oxygen demand
DNA – Deoxyribonucleic acid
dNTP – Deoxynucelotide triphosphate
EBPR – Enhanced biological phosphorus removal
EMB – Eosine methylene blue agar
fg - Femtogram ($1 * 10^{-15}$ g)
MA – Marine agar
MAC – MacConkey agar
MAP – Marine phosphate agar
MSA – Mannitol salt agar
NA – Nutrient agar
NBRIP - National Botanical Research Institute's phosphate growth medium
PAO – Phosphate accumulating organism
PCA – Plate count agar
PCR – Polymerase chain reaction
PCR – Polymerase chain reaction
PHA - Polyhydroxyalkanoate
PHB - Polyhydroxybutanoate
PPK – Polyphosphate kinase
PPX - Exopolyphosphatase
RNA – Ribonucleic acid
SWW – Synthetic wastewater
TBE – Tris/Borate/EDTA
TCA – Tricarboxylic acid cycle
TSS – Total suspended solids
UWWTD - Urban wastewater treatment directive
VFA – Volatile fatty acid
WWTP – Wastewater treatment plant

1 Introduction

Large amounts of wastewater are generated every day in the world. In 2020, it was estimated that globally 380 billion cubic meters were produced annually. Wastewater contains large quantities of nutrients, including, but not limited to 16.6 million tons of nitrogen, 6.3 million tons of potassium and 3.0 million tons of phosphorus. These nutrients are all important components of fertilizer used in agriculture, and their total recovery from wastewater could offset 13.4% of annual agricultural demand globally (Qadir et al., 2020). Additionally, wastewater contains numerous biochemical substances, like proteins, organic acids, sugars, fats and fibers, as well as hormone disruptors, heavy metals, drug residues and more (Huang et al., 2010; Zhao, M. et al., 2016). There are various sources of wastewater which contain various amounts of these substances. Wastewater is generally distinguished into four categories: rainwater, domestic wastewater, agricultural water and industrial wastewater. Wastewater generated by industry normally contains the most pollution, whereas agricultural water is often heavily loaded but the substances it contains are easily biodegradable (Crini & Lichtfouse, 2018). Global approximations show that around 48% of wastewater is released untreated to the environment (Jones et al., 2021). High loads of untreated wastewater in water bodies can cause accumulation of nutrients and eutrophication which can result in depletion of oxygen and consequently, death of organisms in local ecosystems (Preisner et al., 2020; Smol et al., 2020).

1.1 Phosphorus as a resource

The nutrient recovery from wastewater is an important issue, especially regarding phosphorus, which is an essential nutrient for all organisms and vital for the existence of humanity. The element is involved in a number of critical biological processes, for example, it is an important component of adenosine triphosphate (ATP) and other energy-rich compounds, which transfer biochemical energy in cells. Additionally, it is a crucial part of the structure of DNA and RNA molecules, as phosphate esters make up the backbone of the helix strands. Moreover, phosphorus is a component of phospholipids' structure, which make up cell walls and

membranes (Peacock, 2021). In plants, phosphorus is also essential to photosynthesis and respiration. A deficiency of the nutrient inhibits normal plant growth and reduces agricultural crop yields. This is often a limiting factor for primary production, both in agricultural systems and ecosystems (Lambers, 2022).

The natural cycling of phosphorus differs from that of other nutrients in that it is relatively simple and slow. Additionally, the cycle has no significant gaseous compounds and thus, phosphorus has no link from ocean to land. A large proportion of phosphorus is bound as apatite minerals in the Earth‘s crust, significantly limiting its biological availability. The cycling of phosphorus in ecosystems is rather conserved due to the element’s limited nature, indicating that the transfers between soil and biota within the system are larger than what is gained or lost across the system border. Chemical weathering of apatite rocks provides slow but steady input of biologically available phosphorus into terrestrial ecosystems (Yuan, Z. et al., 2018), usually in the form of orthophosphate (PO_4^{-3}) (Paytan & McLaughlin, 2007). There, it travels back and forth between soil and living organisms through food web connections (Yuan, Z. et al., 2018). The world‘s soils hold around 90-200*10^3 million tons of phosphorus, only a fraction of which is available to the biota, since the solubility of phosphorus compounds in soil depends on its pH (Liu, Y. & Chen, 2008).

Phosphorus is lost from terrestrial ecosystems, mainly by soil erosion and surface runoff from land. This delivers phosphorus to rivers, and eventually to oceans, where it enters food webs and accumulates in sediments on the ocean floor (Yuan, Z. et al., 2018). The world‘s oceans contain approximately 27-840*10^6 million tons of phosphorus, thereof, 80-120*10^3 million tons are found in the seawater while the rest is accumulated in sediments. Phosphorus exits marine ecosystems through a small but constant sinking of organic matter to the seafloor, where the phosphorus forms insoluble calcium phosphate. Over time, the sediments are turned into sedimentary rocks due to geological pressure. When phosphorus has become a part of the Earth‘s crust through sedimentation, it takes hundreds of millions of years for tectonic uplift to deliver it back to the surface where weathering can occur, making it available to the ecosystem again (Liu, Y. & Chen, 2008). The cycling of phosphorus in nature is shown in Figure 1.

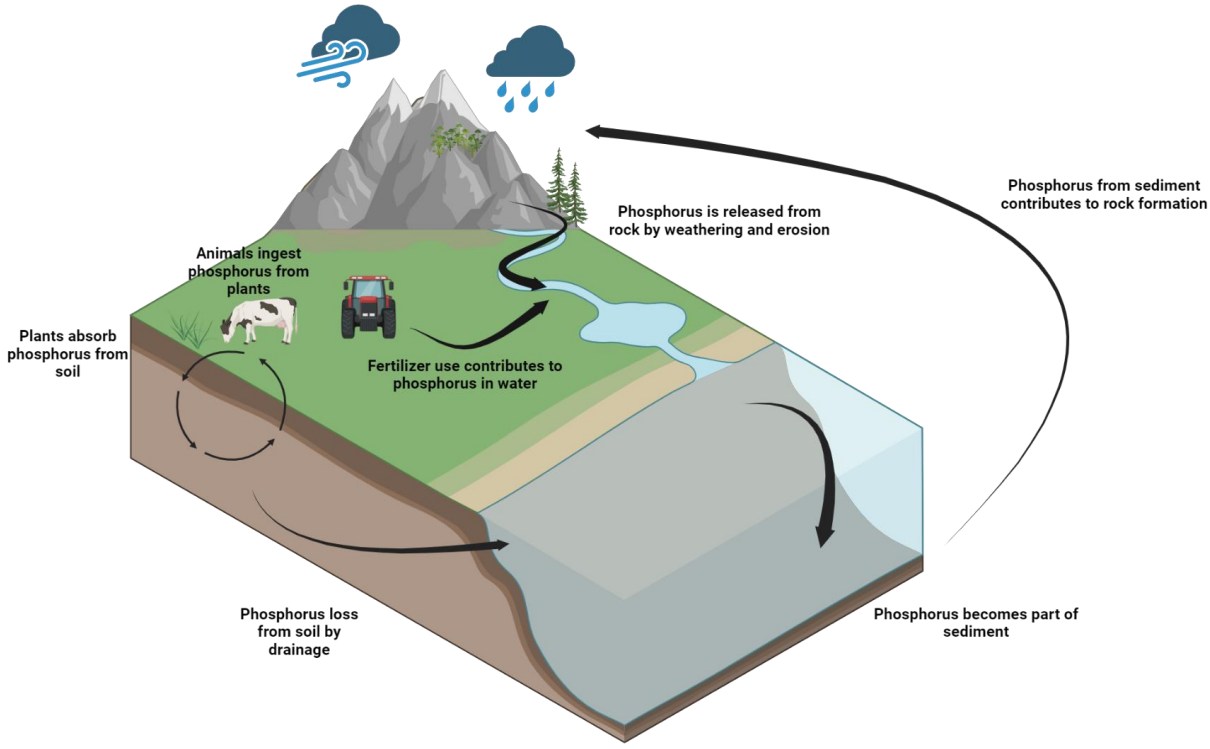

Figure 1: The natural phosphorus cycle. Created with BioRender.com.

Human activities have disrupted the phosphorus cycle by drastically increasing the input to terrestrial systems by mining phosphate rock and applying commercial fertilizers to fields. It is estimated that fertilizer use has doubled or tripled the inflow of phosphorus to freshwaters and oceans compared to prehuman times, elevating the risk of eutropication in water bodies, leading to algal blooms, fish death and water quality impairment (Liu, Y. & Chen, 2008; Yuan, Z. et al., 2018). In 2015, it was estimated that the global phosphorus fertilizer use was approximately 21 million tons per year, and future estimations suggested that by 2050, the demand will have increased to 26 to 39 million tons annually (Bindraban et al., 2020). The growing demand of phosphorus in fertilizers has resulted in a cost increase of phosphate rock from 80$/U.S. ton in 1961 to 700$/U.S. ton in 2015 (1 U.S. ton equals 907.2 kg). In 2007 and 2008, the phosphate rock fertilizer demand exceeded the supply, causing a 400% increase in price in 14 months, denoting the vulnerability of this market (Alewell et al., 2020). Phosphorus is a finite resource which is being depleted. Phosphorus is mined from phosphorus rock and estimations have suggested that the phosphorus in the mines will be depleted in the next decades or centuries. Only a few countries control all of the phosphorus mines in the world, for example, around 75% of all remaining phosphorus mines are found in Morocco (Cordell &

White, 2015). This can cause problems and political conflicts, as those countries are already cutting back on production or export of the nutrient. These issues lead to high cost of phosphorus and, eventually, depletion of the resource. This is why phosphorus management has to improve globally (Chrispim et al., 2019; Cordell & White, 2015; Nedelciu et al., 2020). Because of the emerging phosphorus shortage, alternate sources of phosphorus have gained attention recently, such as mining phosphorus from marine sediments with the aid of microorganisms (Cakmak et al., 2022). Another alternative source of phosphorus is wastewater, which has gained increased attention in recent years (Jones et al., 2021).

1.2 Wastewater treatment

Around half of all wastewater generated globally is treated, both to decrease its negative impacts on the environment, as well as retrieve valuable substances from it (Jones et al., 2020). The effectiveness of wastewater treatment is typically assessed using a number of universal parameters, the most important ones being biochemical oxygen demand (BOD, also referred to as BOD_5), chemical oxygen demand (COD) and total suspended solids (TSS). BOD is a measure of organic material pollution in water, determining the amount of dissolved oxygen consumed by areobic microorganisms as they break down organic matter over a 5-day period at 20°C. COD measures the quantity of organic matters in water, both biologically available and inavailable and is thus typically higher than BOD. It is an estimate of the quantity of oxygen required to oxidise the organic matter present, using a strong chemical oxidising agent, either potassium dichromate or potassium permanganate (Khan & Ali, 2018; Woodard & Curran Inc., 2006). TSS refers to all solids, both dissolved and nondissolved, that do not pass through a 0.45-micron filter (Woodard & Curran Inc., 2006). TSS can include pollutants such as metals, nutrients and hydrocarbons. This is an important parameter, as excessive TSS can lead to a depletion of dissolved oxygen in the effluent (Verma et al., 2013; Zhao, H. et al., 2022). Additionally, wastewater effluent is frequently assessed for total phosphorus and nitrogen concentration as these elements are important and limiting nutrients for algae growth. To prevent eutrophication, it is important to measure and control the amounts of these nutrients in wastewater effluents (Di Capua et al., 2022).

There are numerous ways to treat wastewater, including biological, chemical and physical treatments. The setup of conventional treatment plant is divided into primary, secondary and tertiary treatment. An example of a typical setup is shown in Figure 2. The primary treatment is divided into two steps: preliminary treatment and sedimentation process. The preliminary treatment's purpose is to remove large particles and suspended substances from the effluent, using screens (to remove large solids such as plastic, cloth and paper), grit chambers (to remove grit like sand, broken glass and metal fragments) and skimming tanks (for fatty substance removal). Preliminary treatment does typically result in some reduction in TSS and BOD. In the sedimentation step, primary settling tanks (also referred to as primary clarification tanks) are employed to remove the remaining organic matter and particles from the wastewater via gravity. This is done in order to further lower the oxygen demand of the final effluent that gets fed into receiving water bodies. The water is left undisturbed in the tank for a few hours, during which heavier particles settle down and form so-called primary sludge, which is transferred to a sludge digester. Chemical sedimentation may be used to deposit lighter particles, using coagulants such as alum, ferric chloride and ferric sulfate. The primary treatment typically reduces the BOD of the influent by 20-65% and the TSS by 50-80% (Crini & Lichtfouse, 2018; Gedda et al., 2021; Kesari et al., 2021).

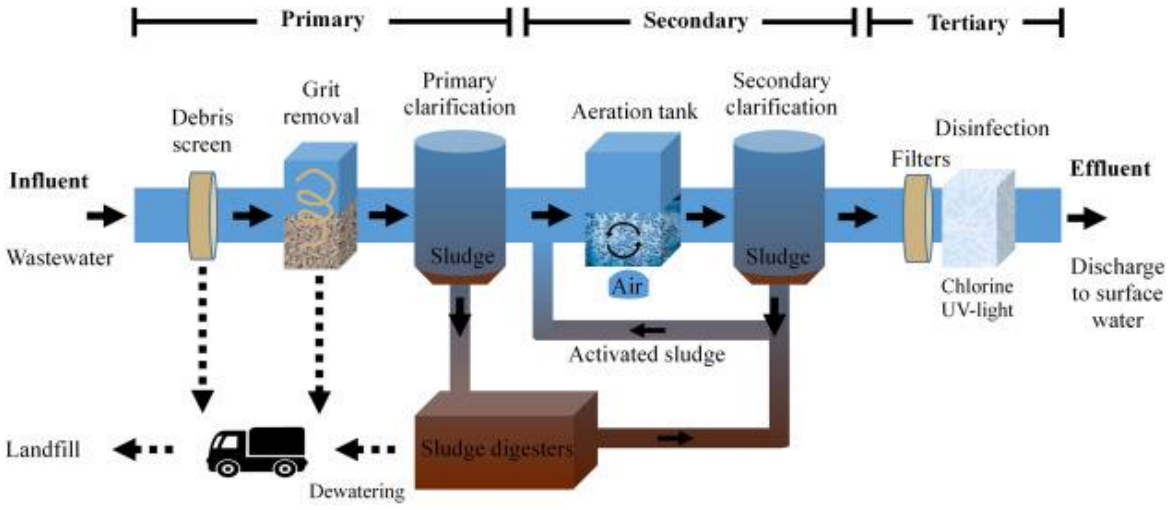

Figure 2: Conventional wastewater treatment plant with primary, secondary and tertiary treatment steps (Genesis Water Tech, 2023).

In the secondary treatment process, microorganisms are employed to degrade organic compounds, which decreases the BOD further. Various types of aerobic systems exist, the most prominent is an activated sludge process where wastewater is fed into an aeration tank, in

which aerobic organisms brake the organic material down (Gedda et al., 2021). After aerobic microbial degradation, the wastewater flows into a secondary clarifier tank, where microbial cells, organic matter, inorganic substances and aggregates settle out and generate activated sludge (Mitraka et al., 2022). Here, chemical coagulation may be necessary to precipitate remaining organic matter and nutrients (Zhang, C. et al., 2022). In addition, the removal of phosphorus and nitrogen can be a part of the secondary treatment process. Nitrogen is mainly present in the form of ammonium in wastewater. During a process called nitrification, ammonia (NH_3) is converted to nitrite (NO_2^-) or nitrate (NO_3^-) under aerobic conditions. In a subsequent anaerobic process called denitrification, the nitrite and nitrate get reduced to N_2, removing biologically available nitrogen and returning it to the atmosphere (Thakur & Medhi, 2019). This can be coupled with the removal of phosphorus in systems that incorporate anaerobic and aerobic conditions to enhance the biological phosphorus removal, as discussed in section 1.2.1 below.

The activated sludge generated in the secondary treatment process is combined with the primary sludge in the sludge digester, where it undgergoes anaerobic digestion during which biogas (CH_4 and CO_2) is generated from organic compounds by methanogens and other microbes. The CO_4 may be collected and used as an energy source. Additionally, anaerobic digestion of the sludge reduces its volume and pathogen numbers (Nabaterega et al., 2021). After microbial digestion, the sludge is dewatered and used as fertilizer or disposed of in landfill (Kesari et al., 2021). The composition of dewatered sludge is variable but on average it contains 50-70% organic matter, 30-50% mineral components, 3.4-4% nitrogen and 0.5-2.5% phosphorus (Rorat et al., 2019).

Lastly, tertiary treatment may be empoyed to further reduce the amounts of phosphorus, nitrogen, remaining biodegradable organic matter, pharmaceuticals, heavy metals and pathogens where the secondary treatment fails to sufficiently do so. Numerous methods exist, for example disinfection via chlorination or ultraviolet radiation, membrane filtration to remove microbial cells, organic compounds, nutrients and/or pharmaceuticals (depends on the method and membrane pore size) and constructed wetlands and microalgae cultivation to further lower the BOD and nutrients such as phosphorus and nitrogen (Gedda et al., 2021; Zagklis & Bampos, 2022).

1.2.1 Enhanced biological phosphorus removal

Some wastewater treatment plants (WWTP) implement enhanced biological removal (EBPR) to the secondary treatment step in the treatment process. This refers to putting the wastewater through a certain set of conditions which favor the growth of a special type of organisms called phosphate accumulating organims (PAOs)(see chapter 1.2.2). EBPR systems are both environmentally friendlier than non-EBPR systems and more efficient at removing phosphorus. Plants with EBPR can remove 85% or more of intitial phosphorus concentration in influent, compared to 15 to 30% of phosphorus removed via microbes in plants without EBPR. Instead, non-EBPR systems may rely on chemical coagulation with Fe(III) and Al(III) salts if a complete P removal is required. This can either be a part of the secondary or the tertiary treatment (Zhang, C. et al., 2022). The sludge derived from chemical coagulation is not recommended as fertilizer since the salts can reduce P mobilization in soils, making it less available to the biota. Instead, the sludge is often burnt or disposed to landfill, which might ultimately lead to contamination of water bodies. However, the usage of sludge derived from EBPR systems as fertiliser is also problematic, because of high contents of heavy metals and radioactive elements, which is toxic to organisms (Zhang, C. et al., 2022). Methods to decrease the heavy metal contents, such as thermochemical treatments with HCl, can be employed but they further increase the cost of phosphorus recovery from wastewater (Havukainen et al., 2016).

EBPR systems can have various setups but typically will include two different zones, one anaerobic and one aerobic. To begin with, the influent wastewater flows into the anaerobic zone, where phosphates are released into the wastewater by PAOs in the sludge, which also take up carbon substrates (mainly volatile fatty acids) from the wastewater and store as polyhydroxylakanoates (PHAs). The wastewater, along with the sludge, then flows to an aerobic zone, where the PHAs are degraded and used for cellular growth and phosphate accumulates intracellularly (Serafim et al., 2002). The sludge is then recirculated and mixed with new influent wastewater. More phosphate is accumulated from the wastewater in the aerobic phase than was initially released by the PAOs in the anaerobic phase. This results in an efficient phosphorus removal from the wastewater, as the effluent has a very low phosphorus content. Phosphates accumulated by the PAOs can get as high as 15% of their dry cell weight (Izadi et al., 2020).

1.2.2 Phosphate accumulating organisms

PAOs, or phosphate accumulating organisms, are a group of microorganisms that can remove phosphorus from wastewater in concentrations that are higher than are required for their normal functioning (also referred to as luxury phosphate uptake). Additionally, they take up volatile fatty acids, like acetate and propionate, under anaerobic conditions and store them as polyhydroxyalkanoates (PHAs) (Dorofeev et al., 2020). PHAs are biodegradable polyesters produced by various microorganisms as an energy reserve. Different types of PHAs exist, among the most promising is polyhydroxy butyrate (PHB), which has many properties in common with conventional plastics. PHB is produced under low levels of oxygen, nitrogen, phosphorus, sulfur or trace elements and high concentrations of carbon. When nitrogen concentration is limited, protein synthesis stops and PHB is produced (Sathya et al., 2018). The ratio between carbon and phosphorus in the media is referred to as C/P ratio and the ratio between carbon and nitrogen is referred to as C/N ratio. It has been reported that both high C/P and C/N ratios promote PHA production, for example 750 and 125, respectively (Wen et al., 2010).

PAOs take up phosphates from the environment and produce PHAs through a cycle that contains two phases. The first phase is anaerobic, during which organic matter is consumed and phosphates are released by the bacteria (Dorofeev et al., 2020). Anaerobic conditions are stressful for PAOs, and as a response to the stress, they will take up carbon from the environment and store it in order to survive a potential long-term period of oxygen deprivation. The primary carbon source in wastewater is acetate, which is transformed into Acetyl-CoA by the PAOs. The energy needed for this reaction is provided by the hydrolysis of ATP, leading to the formation of ADP and a free phosphate group, which is released into the medium. Acetyl-CoA is then converted to PHAs (Tarayre et al., 2016). This process is shown in Figure 3.

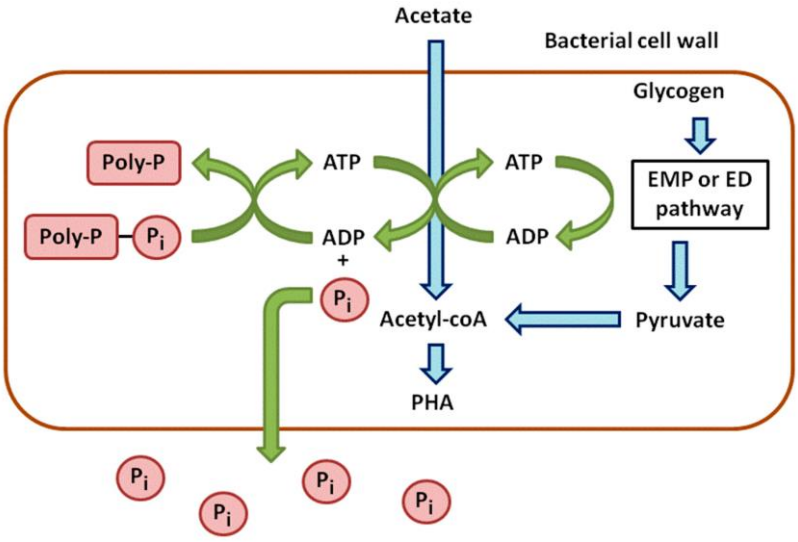

Figure 3: Anaerobic phase of phosphate uptake by PAOs. Acetate from wastewater is taken up and converted into PHA. This requires energy from ATP, leading to release of phosphates to the wastewater (Tarayre et al., 2016).

During the second phase, which is aerobic, oxygen enters the system and serves as an electron acceptor, leading to the uptake of phosphates from the environment (Dorofeev et al., 2020). In this phase, PHAs are degraded into Acetyl-CoA, which go through the tricarboxylic acidcycle (TCA cycle), generating energy and carbon for cell growth (Tarayre et al., 2016). The TCA cycle serves as a metabolic pathway employed by aerobic organisms to produce cellular energy and intermediate molecules for biosynthetic processes (Eniafe & Jiang, 2021). Some of the energy produced in this process is used to take up phosphates from the medium and combining them with ADPs to form ATPs (Tarayre et al., 2016). The process is shown in Figure 4.

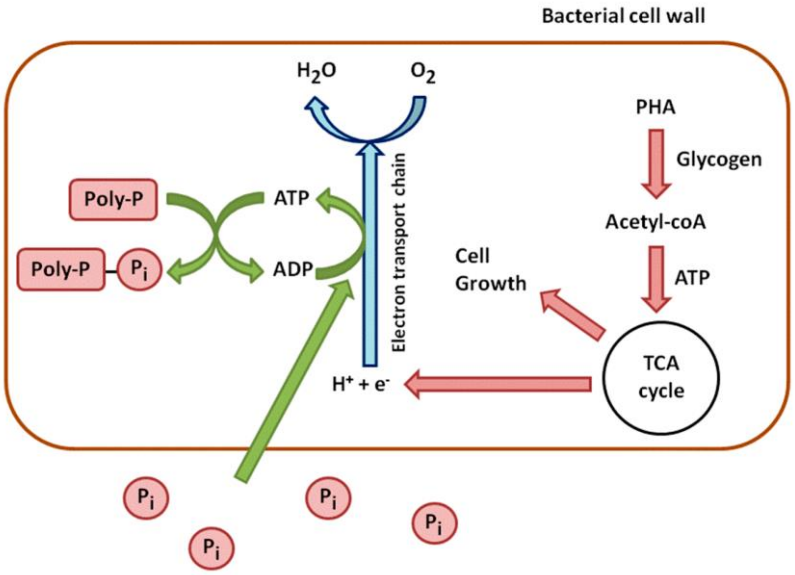

Figure 4: Areobic phase of phosphate uptake by PAOs. Intracellular PHA is broken down to give the cell energy and carbon for growth. The energy is also used to take up phosphates from the wastewater and produce ATP (Tarayre et al., 2016).

Knowledge about the microbial community in EBPR sludge remains rather limited, it is a diverse community comprised of a few prominent bacterial strains. The most studied PAOs are members of the group *Candidatus* Accumulibacter, which belongs to the family *Rhodocyclacea* and the class Betaproteobacteria. There are two main groups within *Ca.* Accumulibacter, both of which are divided into a few clades. The clade composition in sludge is influenced by the types of WWTPs and nutrition conditions (Dorofeev et al., 2020; Izadi et al., 2020). Another group of PAOs commonly present in EBPR sludge are members of the genus *Tetrasphaera*, which belongs to the family *Intrasporangiaceae* of the class Actinomycetes (Havukainen et al., 2016). *Tetrasphaera* members are often found in higher abundances (up to 30% of biomass) than *Ca.* Accumulibacter (up to 20% of biomass) (Onnis-Hayden et al., 2019).

The metabolism of *Tetrasphaera* is not fully consistent with the classical biochemical previously described PAO model, as they can take up and store diverse organic substances such as glucose and amino acids, rather than mainly relying on volatile fatty acids (VFAs) like *Ca.* Accumulibacter. Their PHA production is dependent on the clade composition, but is not as consistent as that of *Ca.* Accumulibacter. *Tetrasphaera* members can supply VFAs for other PAOs, contributing to synergistic interactions for P removal. High *Tetrasphaera* abundances can lead to over 50% of the P removal in WWTPs (Nguyen et al., 2023). Additionally, PAOs have been found in environments with extreme conditions such as the high salinity of the oceans.

These strains can be valuable for phosphorus removal from mariculture wastewater (Zhang, Y. et al., 2024), as well as recovering phosphorus from sediments on the bottom of the ocean (Cakmak et al., 2022).

The key genes that have been attributed to PAOs activity are the polyphosphate kinase gene (*ppk*) and exopolyphosphatase gene (*ppx*) (Xie et al., 2024). Polyphosphates are linear polymers composed of tens to hundreds of phosphate residues, held together by energy-rich phosphoanydride bonds (Achbergerova & Nahalka, 2011). Polyphosphate kinase (PPK) is an enzyme that catalyzes polyphosphate formation from phosphates and exopolyphosphatase (PPX) is an enzyme that catalyzes the hydrolysis of polyphosphates to phosphates. In addition, the inorganic phosphate transporter gene (*pit*) and the high-affinity phosphate transporter gene (*pst*), whose products play a role in cellular phosphate transport, are an important feature of PAOs. These genes are indispensable for PAOs activity, although their presence does not guarantee luxury phosphate uptake, as they are widely preserved in the bacterial domain, including in the genomes of non-PAOs. Thus, identifying the signature genes specific to PAOs remains a challenge (Xie et al., 2024).

It has been proposed that PAOs owe their phosphate accumulating traits to a disorder in the Phosphate regulon (Pho regulon) (Xie et al., 2024), which is a universal regulatory mechanism involved in bacterial phosphate management. The Pho regulon influences the expression of *pst* and *pit*, among other things (Santos-Beneit, 2015). In *Ca.* Accumulibacter, a dysregulation in the Pho regulon causes ineffective regulation of *pst*, leading to excessive phosphate uptake. To prevent phosphate poisoning, the excess phosphate is converted to polyphosphates with PKK2. The PKK2 gene and PhoU gene (a Pho regulon component affecting the expression of *pst*) were derived from different donor bacteria evolutionally, and as a result they have unmatched activation and inactivation thresholds. PKK2 has a tendency to decrease the amount of intracellular phosphate to levels that components of the Pho regulon interpret as low phosphate conditions, encouraging ongoing phosphate uptake (Xie et al., 2024).

1.3 Wastewater treatment in Iceland

Wastewater treatment in Iceland is subjected to regulation 798/1999 concerning drainage systems and sewage, adopted from the European Union in 1999 (directives 98/15/EC and 91/271/EEC) (Reglugerð um fráveitur og skólp nr. 798, 1999). As defined in the regulation, preliminary treatment is the process of removing large particles and objects from the wastewater using a filter or grid, for the purpose of preventing visual impact. Primary treatment requires reduction of the BOD_5-value by at least 20% and suspended solids by at least 50%. Secondary treatment often involves biological treatment followed by precipitation, but various methods can be considered a secondary treatment. According to the regulation, the standard wastewater treatment method is secondary treatment. However, if the receiving water body is defined as “less sensitive”, primary treatment is required as a minimum treatment method (Reglugerð um fráveitur og skólp nr. 798, 1999). For example, a receiving body of water may be classified as “less sensitive” if it has been shown that its water renewal time is only a few days, as is the case with fjord of Eyjafjörður discussed below.

Even so, 14% of wastewater in Iceland remains discharged without treatment, 83% is only treated with preliminary treatment, 1% gets primary treatment and 2% gets secondary treatment (Umhverfisstofnun, 2023), as is shown on Figure 5. As Iceland is not a member of the EU, failure of individual municipalities to comply with the EU Urban Waste Water Treatment Directive (UWWTD) has close to no legal repercussions. Furthermore, talks of more stringent wastewater treatment have been locally met with some pushback, mostly due to high investment cost. The benefits of increased treatment are said to be ”limited” and not worth the expenditure of taxpayer money (Samorka og Samband íslenskra sveitarfélaga, 2020). Member States, however, seem to be closely monitored by the European Commission and can be refered to the EU Court of Justice for not complying with the UWWTD. Most recent examples include that of Poland, Italy, and Spain (European Commission, 2022; European Commission, 2023; European Commission, 2024).

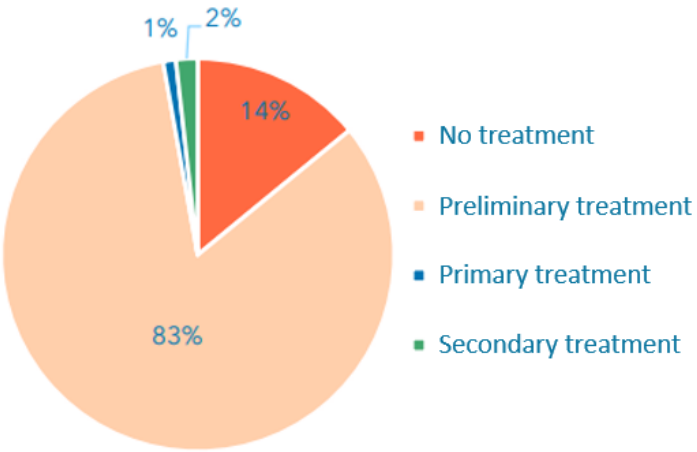

Figure 5: Types of wastewater treatments in Iceland with regard to number of population (Umhverfisstofnun, 2023).

1.3.1 The case of Akureyri (NE Iceland)

The town of Akureyri is located towards the bottom of the fjord of Eyjafjörður in Northeastern Iceland and is frequently referred to as the "capital of North Iceland" as it is the largest municipality outside of the southern Capital Region. As of January 2024, the town's population was just south of 20.000, reaching 86.000 population equivalents (Umhverfisstofnun, 2023). Wastewater from Akureyri is released into the fiord, Eyjafjörður, which remains defined as a less sensitive water body and therefore primary treatment is considered sufficient. However, the wastewater currently only undergoes preliminary treatment, in the form of grit settling and bar screening. Thus, the plant does not fully reach the minimum requirements for primary treatment – that is, a minimum decrease of 20% and 50% in BOD and TSS levels respectively – as summarized in a recent report by The Environment Agency of Iceland (Umhverfisstofnun, 2023). The treatment plant in Akureyri has a capacity of up to 750 L/s, and an average flow of 250 L/s which means that, on average, 7.9 gigalitres of wastewater run through the plant yearly (Norðurorka, n.d.a). According to information from the treatment plant, the effluent wastewater contains approximately 3.3 mg/L phosphorus and 15.9 mg/L nitrogen (Norðurorka, 2023). Assuming that the plant runs at full capacity, this adds up to 26,000 kg of phosphorus and 125,000 kg of nitrogen being released into Eyjafjörður annually.

Wastewater treatment in Akureyri, as well as the rest of the country, is challenging due to a number of reasons. The cold climate makes biolocigal treatment a challenge and can aslo impact chemical treatment (Gunnarsdóttir et al., 2013). A majority of the households in the country is heated with geothermal water, which generates considerable amount of effluents

from the district heating and dilutes the influent wastewater (Ingólfur Bender et al., 2021), making the treatment less effective (Thorndahl et al., 2016). Lastly, a large part of the sewage system in the country remains combined (Ingólfur Bender et al., 2021), which also contributes to dilution of the influent wastewater. Urban drainage systems consist of combined and separate sewer systems. In seperate systems, two separate pipes are used to carry wastewater. Sewage from homes and businesses is carried in one pipe, while rainwater is collected in another pipe. Combined systems only have one pipe, where these wastewater streams are combined. Heavy rainfall or snowmelts can cause flooding in the combined systems, leading overflows where a mixture of untreated sewage and rainwater are released into the environment (Li et al., 2018; Mahaut & Andrieu, 2019). A significant part of the sewer system in Akureyri is combined, mainly in the older parts of town. This can be seen on Figure 6, where red color indicates combined pipes, pink indicates rainwater pipes and orange indicates sewer pipes (Norðurorka, n.d.b).

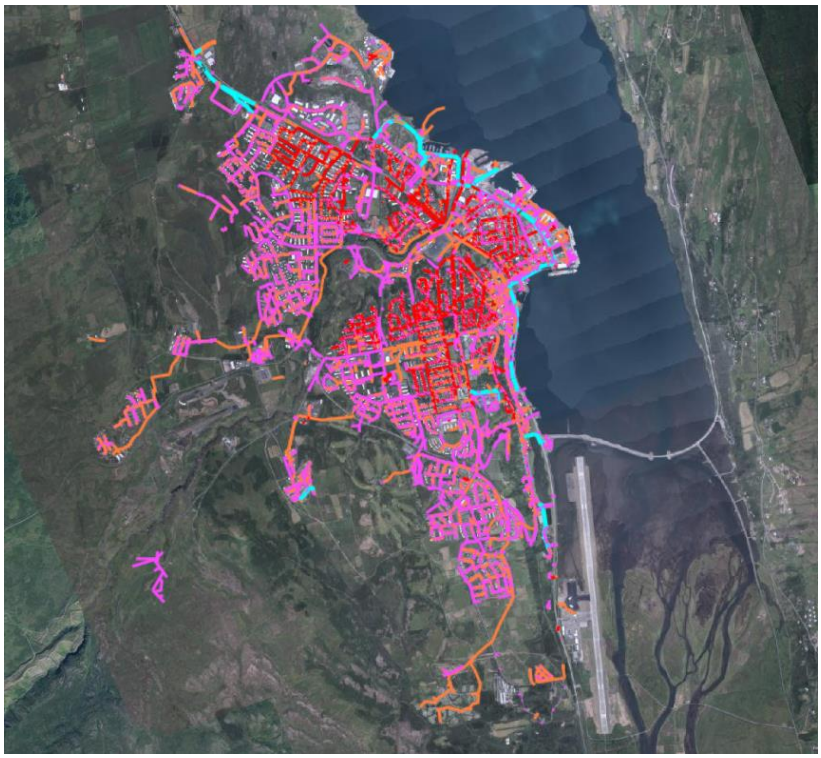

Figure 6: The sewer system in Akureyri (Norðurorka, n.d.b).

1.4 Ecosystem composition of Eyjafjörður

Eyjafjörður is a 60 km long fiord located in the North of Iceland, where the temperate and the frigid zone meet. For this reason, environmental conditions can have drastic and unpredictable variations. This has resulted in less biodiversity in the area compared to other parts of Iceland, as many species adapted to either the temperate or the frigid zone can not live with these environmental variations. Even so, many species are found in the fiord, and are divided into four categories; planktonic taxa, benthos, fish and mammals (Valtýsson & Jónsson, 2000).

The planktonic taxa constitutes of phytoplankton and zooplankton. The phytoplankton, which composes a variety of microalgae species, produce organic materials via photosynthesis, and serve as feed for the zooplankton. Crab fleas are the biggest group of the zooplankton, the most common ones are *Oithona*, *Acartia* and *Calanus finmarchicus*. The zooplankton are an important part of many species‘ diet, such as fish and whales. Some of the most prominent fish species in Eyjafjörður are cod, haddock, American plaice and herring, which are all important for fishing. Mammals in the fiord mainly consist of seals and whales. The four whale species that are commonly seen in the fiord are minke whale and humpback whale, both of which mainly feed on zooplankton, and popoise and white-beaked dolphin, which mainly feed on fish and squids. Benthos are a diverse group of organisms that live on the seafloor, which is rather flat in Eyjafjörður, due to thick sedimentary layers. This group includes macroalgae growing on the seabed, crustaceans, annelida, echinoderms, and molluscs such as snails and bivalves, which are common in the fiord (Valtýsson & Jónsson, 2000).

One of the bivalves found in Eyjafjörður is the Ocean Quahog (*Arctica islandica*) (Valtýsson & Jónsson, 2000), which lives buried into the seafloor at depths ranging from 4 to more than 500 meters. The clam can reach 500 years of age, making it the longest-lived solitary animal on Earth. The species is videly distributed in the entire North Atlantic Ocean, from North Carolina in the USA to Newfoundland in Canada, around Iceland, and along the European coast from Spain to Norway. Due to its longevity and distribution, the science community has found a use for *A. islandica* as a tool in paleoclimatology. As their shell grows periodically throughout life, it contains distinct annual and daily growth increments which can be used to align parts of the

shell to a specific period in time. Changes in the clams' environment influence the increments' width and chemical properties, making it possible to combine information from different specimens into long time-series climate records (Schone, 2013).

Bivalves harbor a diverse community of microorganisms, consisting of fungi, viruses and bacteria, which include members of the families *Proteobacteria*, *Firmicutes*, and *Bacteroidetes*. The microbiota plays an important role in the survival and growth of bivalves and has been found to play a crucial role in nutrient absorption and pathogen defense (Dai et al., 2022; Masanja et al., 2023). The composition of microbial communities varies between different regions of the their body. For example, the gills of clams are dominated by *Proteobacteria*, while the gut is dominated by *Firmicutes* (Masanja et al., 2023). This symbiosis has been found to be beneficial for the clams in question as evidenced by examples of bivalves thriving in otherwise ecologically extreme environments such as hydrothermal vents where the bacterial symbionts provide them with nutrients via chemosynthesis (Duperron et al., 2013). The structure of the bivalve microbial communities is also affected by their habitat, water quality and host species. Bivalves that live in polluted waters can have a different composition of microbiome than those that inhabit unpolluted waters (Masanja et al., 2023). Due to their filter feeding nature, bivalves have been utilized as bioindicators for biomonitoring in aquatic environments for years as chemicals, such as microplastic, heavy metals and genotoxic agents, will accumulate in their soft tissues (D'costa et al., 2018; Ding et al., 2021; Liehr et al., 2005).

1.5 Research background

In this project, clam associated Arctic microbes (CLAAMs) isolated from the gut of ocean quahogs (*Arctica islandica*) were investigated for the ability to produce polyhydroxyalkanoates (PHAs) while removing phosphorus aerobically, in the form of phosphates, from synthetic wastewater (SWW). The quahogs were sampled from Eyjafjörður sediment (Latitude: 65 50.854 N, Longitude 18 11.705 W) in May 2022 and the CLAAMs were subsequently isolated from their gut. Previous work has already identified two promising PHA producers from the culture collection (strains CL131 and CL188) (unpublished data). The goal of this current work was to complete the screening of the CLAAM collection for potential PHA producers and investigate them for their ability to aerobically accumulate phosphate and produce PHAs from SWW. The chemical composition of the SWW was informed by the average composition of the wastewater that runs through the wastewater treatment plant in Akureyri. A schematic drawing of the project is shown in Figure 7.

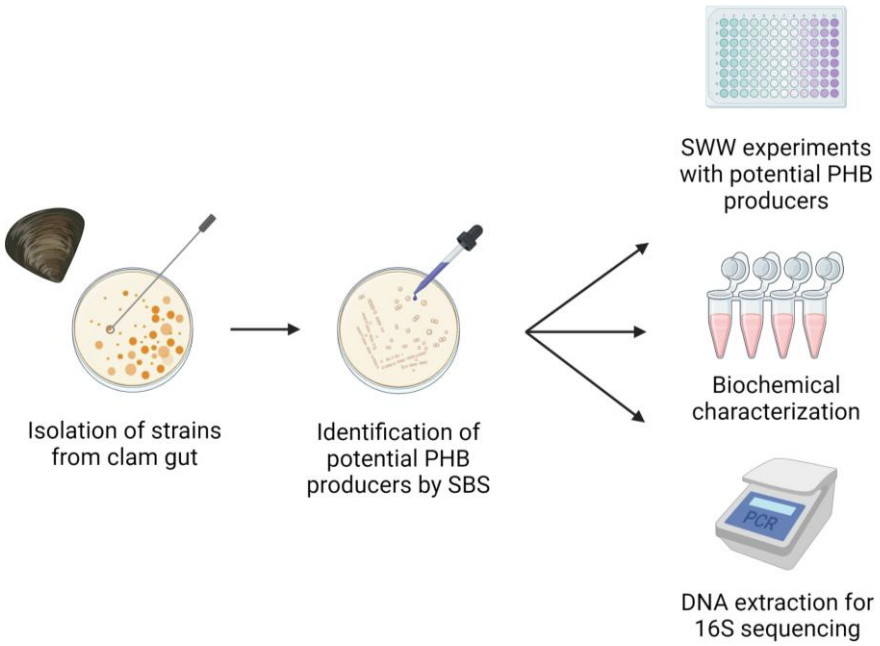

Figure 7: The research shown graphically. Created with BioRender.com.

This study can provide valuable information about the clams' ability to survive in an environment polluted by wastewater, as well as gaining information about how wastewater treatment in Iceland can be improved using locally sampled organisms, as phosphorus uptake from wastewater and its reuse is important to close its ecological circulation. As such, the project supports Sustainable Development Goals nr. 2, 12 and 14 as put forward by the United Nations in 2015 (United nations, n.d.). The aim of Goal 2 is no hunger, which relates to the project as the recovering of phosphorus, which is important nutrient for plants and thus, food security, is addressed. Goal 12 aims at responsible consumption and production, which correlates to this work's focus on closing the phosphorus cycle and increasing responsible food consumption and production. The focus of Goal 14 is to protect life below water, which can be related to the project, since lessening the amount of phosphorus released into water bodies decreases the risk of eutrophication.

In summary, an effort was made to answer the following research questions:

- Can promising PHA producing CLAAMs remove phosphates from synthetic wastewater under aerobic conditions?
- Is there a correlation between PHA production and phosphate removal in CLAAMs?

It is hypothesized that CLAAMs can take up phosphate from SWW while producing PHA, based on existing literature (Dorofeev et al., 2020; Sathya et al., 2018; Tarayre et al., 2016). Furthermore, it is hypothesized that there is a correlation between PHA production and phosphate removal in CLAAMs, based on the literature (Korkakaki et al., 2017).

2 Materials and methods

All reagents were obtained from Sigma-Aldrich unless otherwise noted.

Light absorbance readings were obtained using ClarioStar Plus (BMG Labtech, Germany) unless otherwise noted.

2.1 Selection of promising PAOs

Previosly, a number of ocean quahogs (*Arctica islandica*) were obtained from Eyjafjörður. The molluscs were dissected, their digestive tracts identified, excised and homogenized in sterile basal mineral medium (for medium composition see Table 7 in Appendix). Next, gut homogenates were serially diluted and plated on plate count agar (PCA), nutrient agar (NA), and marine agar (MA) using the spread plate method. Plates were incubated at temperatures varying from 5°C to room temperature to allow for the growth of both psychrophilic/-tolerant bacteria and mesophilic/-tolerant organisms. Pure isolates were obtained by sampling single colonies. Isolates were grown on their preferred solid medium and fresh cultures used to make freezer stocks (30% glycerol).

Strains were reactivated from freezer by streaking one loopful of glycerol stock solution on solid media. In total, 74 strains were streaked onto their respective media (MA, NA or PCA), depending on which type they were initially isolated on. The strains were incubated at room temperature for one week, after which, they were restreaked and incubated for 48 hours as to ensure that fresh cultures were used in experimental work. As PAOs are known for producing PHAs, reactivated strains were assessed qualitatively for their ability to produce PHAs on solid medium as part of the selection process.

2.1.1 Sudan Black staining

Sudan Black staining as described by Liu et al. (1998) and Narayanan et al. (2020), was performed on cultures grown on solid media to screen for intracellular PHA production. Each solid culture was flooded with Sudan Black B (0.05% w/v in ethanol) and let stain for half an hour at room temperature. Staining intensity was evaluated qualitatively via visual assessment

(0, +, ++ or +++). The three strains observed having the highest staining intensity were selected to include in further work, in addition to the two strains already identified as promising PHA producers in previous work (CL131 and CL188).

2.2 Synthetic wastewater experiments

2.3.1 Preparation of SWW and inoculation

Two types of synthetic wastewater were prepared, one was according to OECD guideline 303A (2001) supplemented with sodium acetate as carbon source and the other according to Boeije et al. (1999) (hereafter referred to as Syntho).

Three various phosphate and acetate quantities were tested in the OECD wastewater. The phosphate concentrations were 28 mg/L (160.7 µM) (P1), 56 mg/L (321.5 µM) (P2) and 140 mg/L (803.7 µM) (P3) and the acetate concentrations were 0 mg/L (A1), 120 mg/L (2032.4 µM) (A2) and 240 mg/L (4064.8 µM)(A3). This resulted in C/P ratios ranging from 0 to approximately 18.3. More detailed description of the OECD wastewater components can be seen in Table 10 and Table 11 in Appendix. Four various phosphate and acetate concentrations were tested in the Syntho wastewater. The phosphate concentrations were 23 mg/L (117.3 µM) (P1), 45 mg/L (234.7 µM) (P2), 225 mg/L (1173.4 µM) (P3) and 450 mg/L (2346.8 µM) (P4) and the acetate concentrations were 0 mg/L (A1), 120 mg/L (2032.4 µM) (A2) 1200 mg/L (20,324 µM) (A3) and 12,000 mg/L (203,238 µM) (A4). This resulted in C/P ratios ranging from 0 to approximately 1732. More detailed description of the Syntho wastewater components can be seen in Table 12 and Table 13 in Appendix. Each condition was prepared in an Eppendorf tube containing a final volume of 980 µL.

The SWW was autoclaved at 121°C for 15 minutes. Approximately 20 µL of fresh liquid cultures (24-48 h) of each strain were inoculated into the Eppendorf tubes, the inoculated SWW was then transferred to wells on a Honeycomb 2 microplate and placed in a Bioscreen C (OY Growth Curves, type FP-1100-C) for three days at 20°C and continuous shaking. Optical density of each culture in each well was read at 600 nm every 15 minutes allowing for backend growth curve analysis.

2.3.2 Phosphate assay

To quantify the strains' uptake of phosphate, colorimetric phosphate assay was performed, according to Murphy and Riley's method for determination of phosphate in water (1962) with microplate modifications. Briefly, phosphate standards in the range of 10 µM to 100 µM were prepared by diluting a freshly made 1000 µM stock solution of disodium hydrogen phosphate dihydrate in distilled water. A coloring reagent mixture (CRM) was prepared by mixing 2,5 mL potassium antimony-(III) oxide tartrate hydrate (0.00274 w/v% in distilled water), 7,5 mL ammonium heptamolybdate tetrahydrate (0.04 w/v% in distilled water), 25 mL sulfuric acid (0,14 v/v% in distilled water) (Honeywell Research Chemicals, ref. 30743), and 15 mL ascorbic acid (0.0176 w/v% in distilled water). In a microtiter plate, 100 µL of sample or standard were mixed with 100 µL of distilled water and 32 µL of CRM. The plate was incubated for 20 minutes before reading light absorbance at 880 nm.

2.3.3 PHA assay

Intracellular PHA was measured quantitatively as originally described by Porras et al. (2017), with modifications for microtiter plates. Samples in a 96-well microtiter plate were centrifuged at 4400 rpm for 15 minutes, supernatant discarded with a needle and the pellet washed with 200 µL distilled water. The plate was vortexed at 500 rpm for 60 seconds, after which it was centrifuged at 4400 rpm for 15 minutes and supernatant discarded. The pellets were stained with 200 µL Sudan Black B (0,05 v/v% in absolute ethanol) and shaken at 200 rpm for 20 minutes, after which they were centrifuged at 4400 rpm for 15 minutes. The supernatant was discarded and the pellets were washed twice with distilled water, after which 200 µL of 70% ethanol were added to each well. The plate was shaken at 200 rpm for 20 minutes and centrifuged at 4400 rpm for 15 minutes, after which, 100 µL of supernatant was transferred to a new plate and light absorbance measured at 580 nm. A previously obtained PHA standard curve (0 to 50 µM) was used as a reference.

2.3 Biochemical tests and characterization

The five strains were tested for various biochemical activities to further shed light on their characteristics.

2.3.1 Phosphate mobilization

The strains were grown on phosphate-containing media to check for their abilities to mobilize phophate. The strains that were initially isolated on NA and PCA were grown on NBRIP media (National Botanical Research Institute's phosphate growth medium, see Table 8 in Appendix for composition). Those initially isolated on MA were grown on NBRIP media, supplemented with NaCl (approximately 2%), and MA media supplemented with 5 g/L calcium phosphate heptahydrate (same amount as in NBRIP), hereafter referred to as MAP.

2.3.2 Gram staining and KOH string test

The strains were Gram stained by placing a drop of distilled water on a microscopic slide and smearing a loopful of culture from solid media into the drop. The slides were let air dry completely before heat fixing the smear by passing them through a flame once. The slides were let cool before flooding them with 1% Crystal Violet solution for one minute, after which the stain was poured off. The slides were flooded with Gram‘s Iodine solution for one minute. The slides were washed with ethanol until the eluent was pale violet, before washing them with water. The slides were counterstained with 0.05% (w/v) safranine solution for 30 seconds, washed with water, blot dried and examined under microscope.

KOH string test was performed by placing two drops of 3% (w/v) KOH on a glass slide and smearing a loopful of culture from solid media into the drop for 10 seconds. The development of viscous solution and a string by slowly raising the loop was indicative of a positive test.

2.3.3 Biochemical tests

A total of 11 biochemical tests were performed on the strains, all of which were previously described by Tindall et al. (2007).

1. Catalase activity (H_2O_2)

A loopful of culture was streaked on a glass slide, to which 2 drops of 3% (v/v) hydrogen peroxide were added. The evolution of bubbles indicated a positive test.

2. Arginine hydrolysis, lysine, and ornithine decarboxylation (ARG, LYS, ORN)

A loopful of culture was inoculated into 1 mL of Moller's Broth base supplemented with either 1% (w/v) L-arginine monohydrochloride, L-lysine dihydrochloride or L-ornithine dihydrochloride (see Table 9 in Appendix for media composition). Next, the broth was overlayed with approximately 0.3 mL of sterile paraffin oil and cultures incubated for four days at room temperature. A positive test was indicated by violet or red color.

3. Urease activity (URE)

One drop of 20% (w/v) urea was added to 0.5 mL of Christen urea agar and mixed. The tube was inoculated with a loopful of culture and incubated for 24-48 hours at room temperature. A positive test was indicated by a pink or red-violet color.

4. Citrate test (CIT)

A single streak of culture was made on a tube of Simmon's citrate agar and incubated for four days at room temperature. A color change of the agar, from green to blue, indicated a positive test.

5. VP test (VP)

A loopful of culture was inoculated into 1 mL of methyl-red-Voges-Proskauer (MRVP) broth and incubated at room temperature. After 48 hours, 0.6 mL of 5% (w/v) α-naphthol dissolved in ethanol was added followed by 0.2 mL of 40% (w/v) KOH. The tubes were vortexed and incubated at room temperature for 15 minutes. A strong red color indicated a positive test.

6. Indole test (IND)

A tube of nitrate, nitrite, and carbohydrate free medium containing 0.1% (w/v) L-tryptophan was inoculated with culture and incubated at room temperature for 48 hours, after which, 0.5 mL of Kovac's reagent (consisting of 5 g p-dimethylaminobenzaldehyde in a mixture of 75 mL amyl alcohol and 25% conc. HCl) was added to the tube and shaken. A positive test was indicated by a red color.

7. Methyl red test (MR)

A tube of methyl-red-VogesProskauer (MRVP) broth was inoculated with a loopful of culture and incubated at room temperature for four days, after which, 5 drops of methyl red indicator solution was added. A positive test was indicated by the development of a bright red color.

8. Oxidation-fermentation test (OF)

In a tube (marked as OF-O) containing 0.5 mL Hugh Leifson medium base, 0.3 ml of 10% (w/v) sterile glucose solution were added and mixed. The tube was inoculated with a loopful of culture and inoculated overnight at room temperature. The same procedure was followed for a second tube (marked as OF-F). Additionally, a few drops of sterile paraffin oil were put on top of the inoculum. A positive test was indicated by a yellow color change.

9. Nitrate reduction (NIT)

A loopful of culture was inoculated into Tryptic Soy Broth supplemented with 0.1% (w/v) potassium nitrate and 0.17% (w/v) agar and incubated at room temperature. After 48 hours, a drop of Nitrate Reduction Reagent (consisting of 0.02 g of N-(1-naphthyl)ethylenediamine dihydrochloride dissolved in 100 mL of 1.5 N HCl and 1.0 g sulfanilic acid diluted in 100 mL of 1.5 N HCl) was added to the tubes and incubated for 15 minutes. The formation of a red-purple color indicated nitrite formation. If no red color developed, 5 mg of zinc powder were added. The development of red color indicated no nitrate reduction, while no color formation indicated a complete reduction of nitrate to nitrogen gas.

10. API strips

All strains were tested with the API 20E strip according to the manufacturer's instructions (BioMérieux, n.d.). Briefly, a suspension of each strain was prepared and used to appropriately fill each microtube on the strip. Strips were incubated at room temperature for 48 h after which each tube was evaluated visually.

11. Starch hydrolysis

The strains' ability to hydrolyze starch was tested by streaking on starch agar (nutrient agar with added 2 g/L water soluble starch). After 48 hour incubation at room temperature, all plates were flooded with Gram's Iodine solution and observed for clear halo formation indicative of starch hydrolysis.

2.2.4 Selective isolation media

A loopful of each of the five strains was streaked on Eosin-methylene blue agar (EMB), MacConkey's agar (MAC), Mannitol salt agar (MSA) and Brilliant green agar (BGA) and incubated for five days at room temperature. Plates were then assessed visually for positive reactions with the help of the Difco™ and BBL™ Manual (Zimbro et al., 2009).

2.2.5 Temperature growth range

Each strain was streaked on plates containing its media of isolation and incubated for five days at seven different temperatures, ranging from 5°C to 50°C.

2.4 DNA extraction and PCR

DNA was extracted from the five strains using DNeasy PowerLyser Microbial Kit (Qiagen, ID: 12255-50). Both homogenization options (homogenizing at 2000 rpm for five minutes and vortexing at maximum speed for ten minutes) were used. In addition, the vortexing step was done at 90°C.

Following DNA extraction, 16S PCR was performed in a total volume of 25 µL, containing 2.5 µL 10x buffer, 0.5 µL 27F primer, 0.5 1492R primer, 0.5 µL dNTP, 0.125 µL *Taq* polymerase, 20.375 µL nuclease free water and 1 µL of DNA. Additionally, samples containing the same mixture of reagents, but untreated bacterial colonies instead of the product from DNA extraction, of four strains (CL188, CL197, CL198 and CL242) were run through the PCR in separate wells. This was done as prior attempts to amplify the 16S gene from the bacteria had failed, and the DNA might have degraded during the DNA extraction. The PCR was run for 35 cycles on SimpliAmp Thermal Cycler (Applied Biosystems by Thermo Fisher Scientific, ref. A24812) according to the program 16S_27F_1492R (see Table 16 in Appendix for program specifications). The PCR product underwent electrophoresis on a 1% agarose gel, containing 1 µL SYBR Safe, in 0,5% TBE buffer at 110 V for 35 minutes. The product was then visualized with UV illumination in Ingenius LHR (Syngene Bio Imaging) and subsequently stored at -20°C.

3 Results

Reactivation of the frozen strains was successful in 31 cases of the 74 strains attempted. A list of reactivated strains along with morphology notes can be viewed in Table 14 in Appendix.

3.1 Selection of promising PAOs

All 31 reactivated strains were stained with Sudan Black, dye retention was observed and rated for seven of them, as can be seen in Table 1.

Table 1: Qualitative Sudan Black staining results for strains CL197, 198, 209, 240, 242, 262, and 276. Staining intensity was evaluated as + (lowest), ++ or +++ (highest).

Strain	Result
CL197	+++
CL198	+++
CL209	+
CL240	+
CL242	++
CL262	+
CL276	+

The three strains with the strongest dye retention were chosen for continued work. Figure 8 shows those strains after staining, along with CL131, CL188 and one strain which did not stain, for comparison.

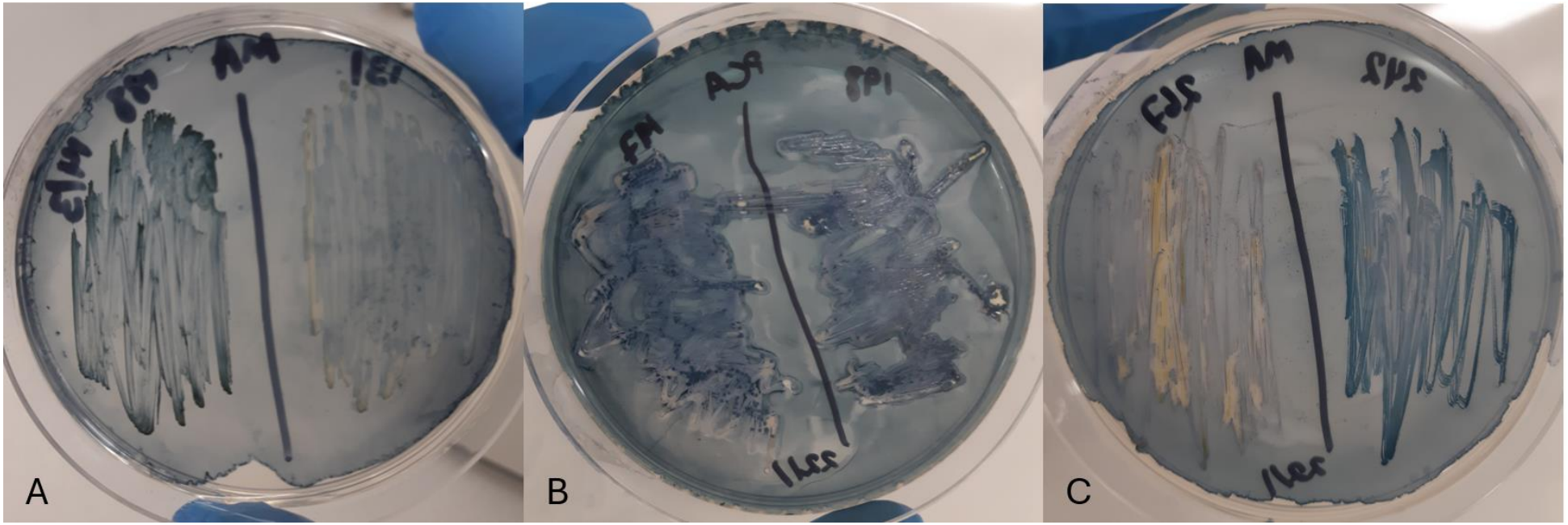

Figure 8: Strains CL131, CL188, CL197, CL198, CL242 and CL267 after Sudan Black staining.

As seen in Figure 8, strains CL197 and CL198 both had spots that stained dark blue while the rest of the colonies stained light blue. The colonies of both CL188 and CL242 stained evenly, while CL131 was only stained vaguely and CL267 did not retain any dye.

3.2 Synthetic wastewater experiments

Each of the five strains was incubated in both OECD (nutrient-poor) and Syntho (nutrient-rich) SWW to assess their phosphate accumulation and PHA production abilities under aerobic conditions. Simultaneously, their growth was analyzed to generate growth curves. No clear exponential or stationary phases were seen in either types of SWW, but they were observed in the strains' broth of isolation (PCB and MB).

3.2.1 OECD SWW: phosphate accumulation

The aerobic phosphate uptake of CL131 in the OECD SWW ranged from 0% to 34.9% of initial phosphate concentration, as can be seen in Figure 9. The initial concentrations of phosphate ranged from 222 µM (P1) to 458 µM (P2) to 1134 µM (P3), while the levels of initial acetate concentrations were 0 µM (A1), 2032 µM (A2) and 4065 µM (A3).

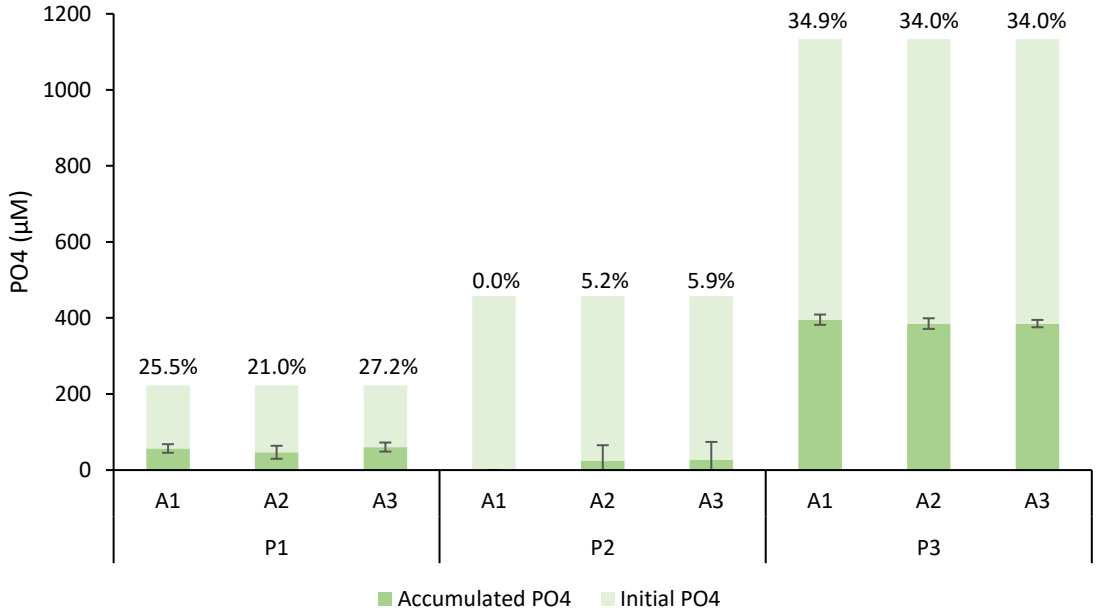

Figure 9: Phosphate accumulation of strain CL131 incubated in OECD SWW for three days at 20°C. Light green columns indicate initial phosphate concentration while dark green columns indicate phosphate levels after incubation. The percentage above the columns represents the proportion of initial phosphate accumulated by the bacterium. P1-3 and A1-3 refer to different initial phosphate and acetate concentrations of the SWW. Values are represented as averages of triplicate measurements with standard deviation depicted as error bars.

As depicted in Figure 9, the amount of phosphate accumulated by CL131 varied between initial phosphate concentrations. The highest amount of phosphate was accumulated in P3 conditions, where the average uptake was around 390 ± 12 µM. This resulted in an uptake of 34 to 35%. The lowest amount of phosphate was accumulated in P2 conditions. On average, the uptake was 17 ± 34 µM and the uptake rate was 0 to 5.9%. In P1 conditions, the average uptake was 54 ± 13 µM, with uptake rates from 21 to 27.2%.

Statistical tests were performed in Jamovi (The jamovi project, 2021) to evaluate the significance of the results. Since the sample size was small, a non-parametric One-Way Anova (Kruskal-Wallis) was performed, which indicated a significant difference between groups incubated under the various phosphate conditions ($p < .001$). A subsequent Dwass-Steel-Crithchlow-Fligner pairwise comparisons (DSCF) post-hoc test showed that there was a significant statistical difference between groups incubated under conditions P1 and P3 ($p = 0.001$) and P2 and P3 ($p < 0.001$).

The phosphate uptake of CL188 in the OECD SWW ranged from 0% to 36.1% of initial phosphate concentration. The strain's phosphate uptake differed with initial phosphate uptake, as can be seen in Figure 10.

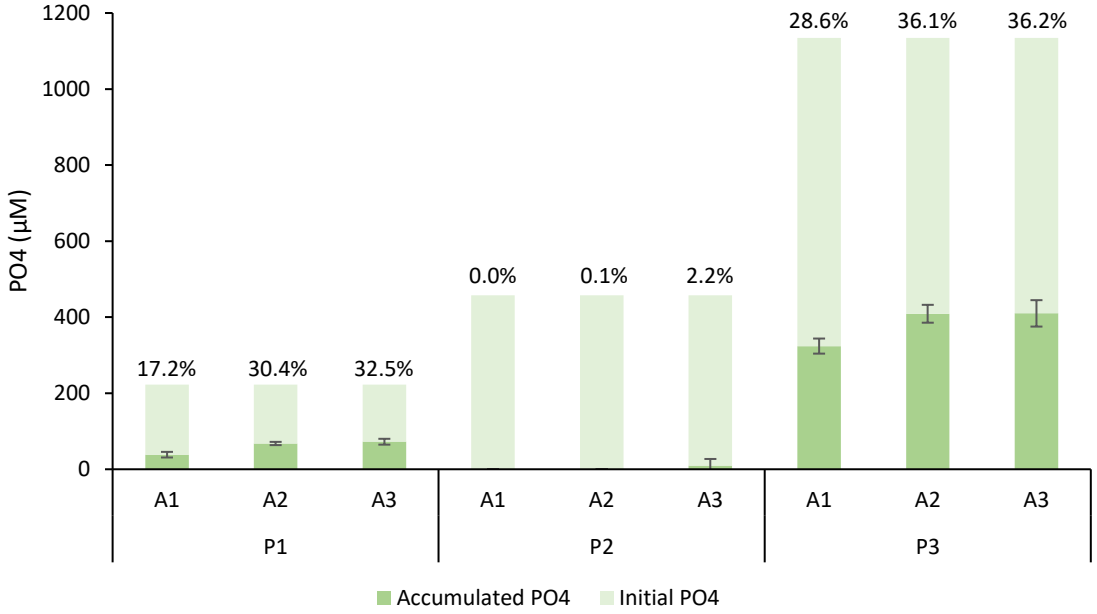

Figure 10: Phosphate accumulation of strain CL188 incubated in OECD SWW for three days at 20°C. Light green columns indicate initial phosphate concentration while dark green columns indicate phosphate levels after incubation. The percentage above the columns represents the proportion of initial phosphate accumulated by the bacterium. P1-3 and A1-3 refer to different initial phosphate and acetate concentrations of the SWW. Values are represented as averages of triplicate measurements with standard deviation depicted as error bars.

On average, the strain was able to accumulate around 381 ± 49 µM of phosphate when incubated in P3 conditions, as depicted in Figure 10. This resulted in uptake rates of 28.6 to 36.2% of initial phosphate concentration. Incubation in P1 conditions resulted in a little lower uptake rates, 17.2 to 32.5%, but a lower accumulated amount, which was on average 60 ± 17 µM. The uptake in P2 conditions was 3.4 ± 10 on average.

As before, the sample size was small so a Kruskal-Wallis test (KW) was performed to evaluate statistical significance. According to the test, there was a statistically significant difference between groups incubated under the three phosphate conditions (p = < 0.001). A subsequent DSCF test revealed that there was a significant difference between P1 and P2 (p = < 0.001), P1 and P3 (p = 0.001), and P2 compared to P3 (p = < 0.001).

In Figure 11, results for the phosphate uptake of CL197 incubated in OECD SWW are shown.

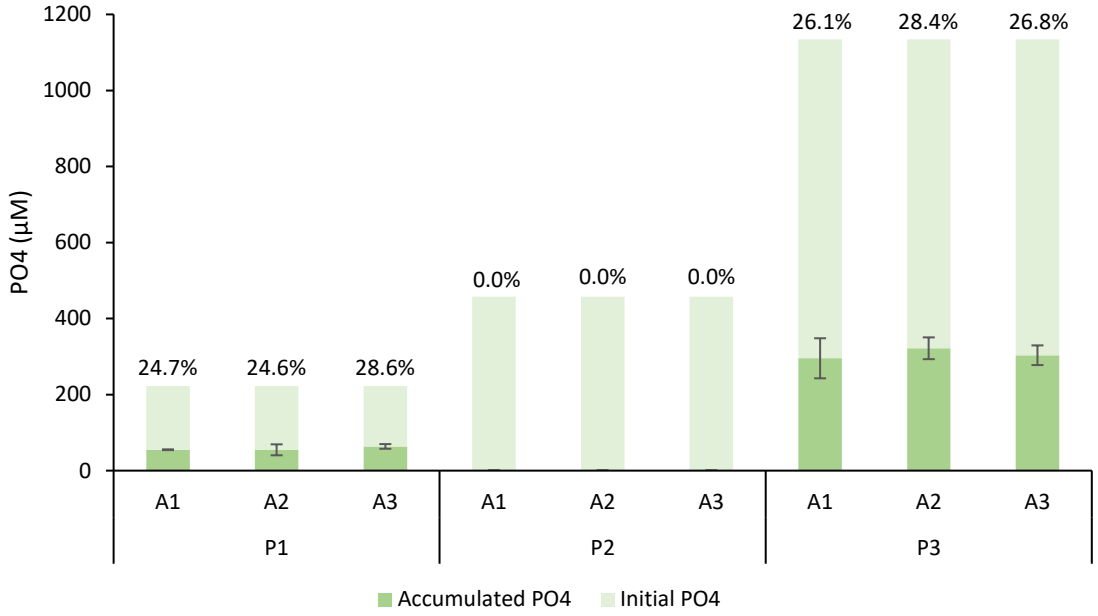

Figure 11: Phosphate accumulation of strain CL197 incubated in OECD SWW for three days at 20°C. Light green columns indicate initial phosphate concentration while dark green columns indicate phosphate levels after incubation. P1-3 and A1-3 refer to different initial phosphate and acetate concentrations of the SWW. The percentage above the columns represents the proportion of initial phosphate accumulated by the bacterium. Values are represented as averages of triplicate measurements with standard deviation depicted as error bars.

As depicted in Figure 11, no phosphate uptake was observed in wells containing P2 SWW. For P1 and P3 conditions, the proportion of uptake was around the same range, from approximately 25% to 29%. The phosphate uptake in P1 conditions was on average 58 ± 9 µM while the average uptake in P3 conditions was 307 ± 35 µM. KW and DSCF tests showed that the difference between P1 and P2 was significant ($p < 0.001$), as well as P1 and P3 ($p < 0.001$) and P2 and P3 ($p < 0.001$).

The phosphate uptake of strain CL198 varied with initial phosphate concentrations, and in some cases it varied with acetate concentrations as well, as seen in Figure 12.

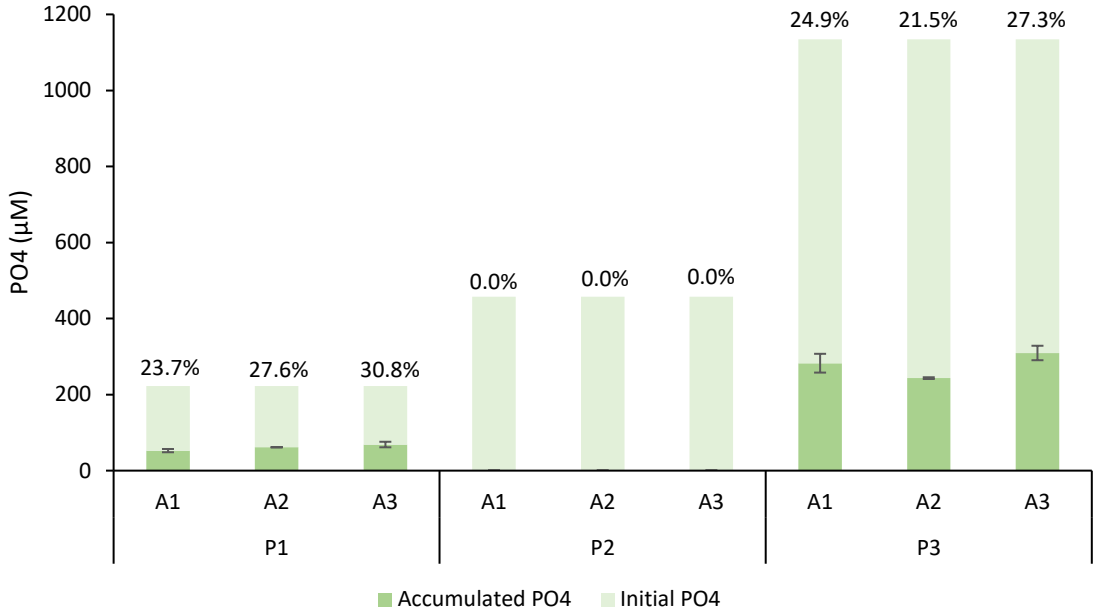

Figure 12: Phosphate accumulation of strain CL198 incubated in OECD SWW for three days at 20°C. Light green columns indicate initial phosphate concentration while dark green columns indicate phosphate levels after incubation. P1-3 and A1-3 refer to different initial phosphate and acetate concentrations of the SWW. The percentage above the columns represents the proportion of initial phosphate accumulated by the bacterium. Values are represented as averages of triplicate measurements with standard deviation depicted as error bars.

The strain's average phosphate uptake was 61 ± 8 µM when incubated under P1 conditions, which resulted in proportion uptake ranging from 23.7 to 30.8%, as depicted in Figure 12. When incubated under P2 conditions, the strain did not seem to accumulate any phosphate, although the growth curves for all phosphate and acetate conditions looked similar. For groups grown under P3 conditions, average phosphate uptake was 283 ± 32 µM. A statistical analysis with KW and pairwise comparisons (DSCF test) confirmed a significant difference between the three phosphate groups, P1 and P2 ($p < 0.001$), P1 and P3 ($p = 0.002$) and P2 and P3 ($p < 0.001$).

In Figure 13, the phosphate uptake of strain CL242 is shown. The phosphate uptake ranged from 0% to 27% and was indfluenced by initial phosphate, and in some cases the acetate concentration.

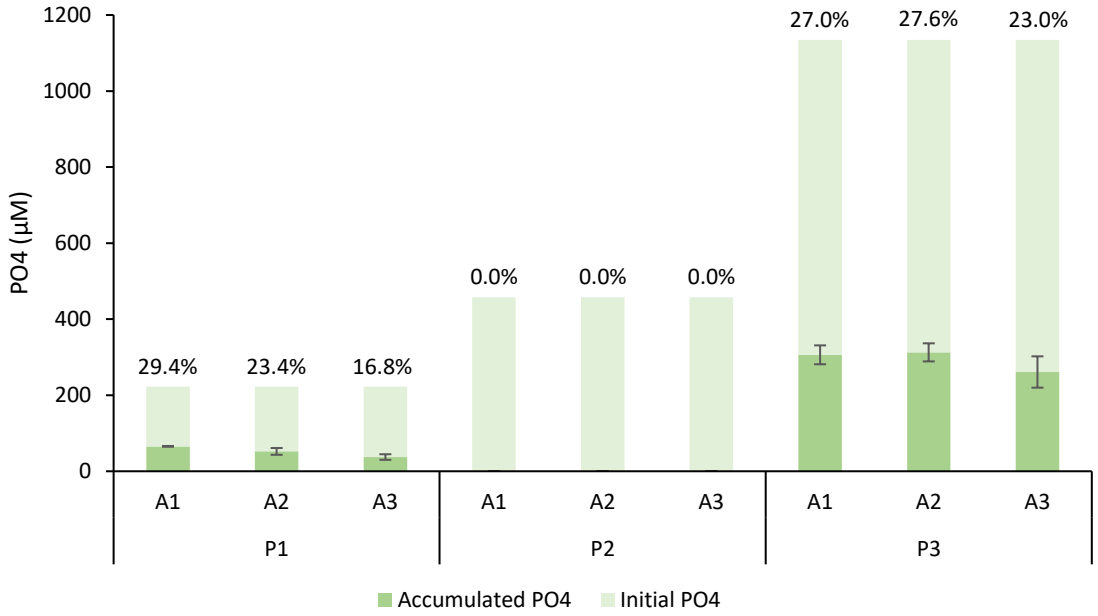

Figure 13: Phosphate accumulation of strain CL242 incubated in OECD SWW for three days at 20°C. Light green columns indicate initial phosphate concentration while dark green columns indicate phosphate levels after incubation. P1-3 and A1-3 refer to different initial phosphate and acetate concentrations of the SWW. The percentage above the columns represents the proportion of initial phosphate accumulated by the bacterium. Values are represented as averages of triplicate measurements with standard deviation depicted as error bars.

When the strain was grown under any of the P2 conditions, no phosphate uptake was measured, as summarized in Figure 13. The average uptake of P1 groups was 52 ± 13 µM while the average uptake of P3 groups was 293 ± 36 µM. The phosphate uptake varied between acetate concentrations within these two groups as well. KW and DSCF pairwise comparisons revealed a significant difference between groups P1 and P2 (p = < 0.001), P1 and P3 (p = 0.001) and P2 and P3 (p = < 0.001).

3.2.2 Syntho SWW: phosphate accumulation

The results for the aerobic phosphate uptake of CL131 in the Syntho SWW is shown in Figure 14. The initial concentrations of phosphate ranged from 166 µM (P1) to 280 µM (P2) to 1557 µM (P3) to 2498 µM (P4), while the levels of initial acetate concentrations were 0 µM (A1), 2032 µM (A2), 20,324 µM (A3) and 203,238 µM (A4).

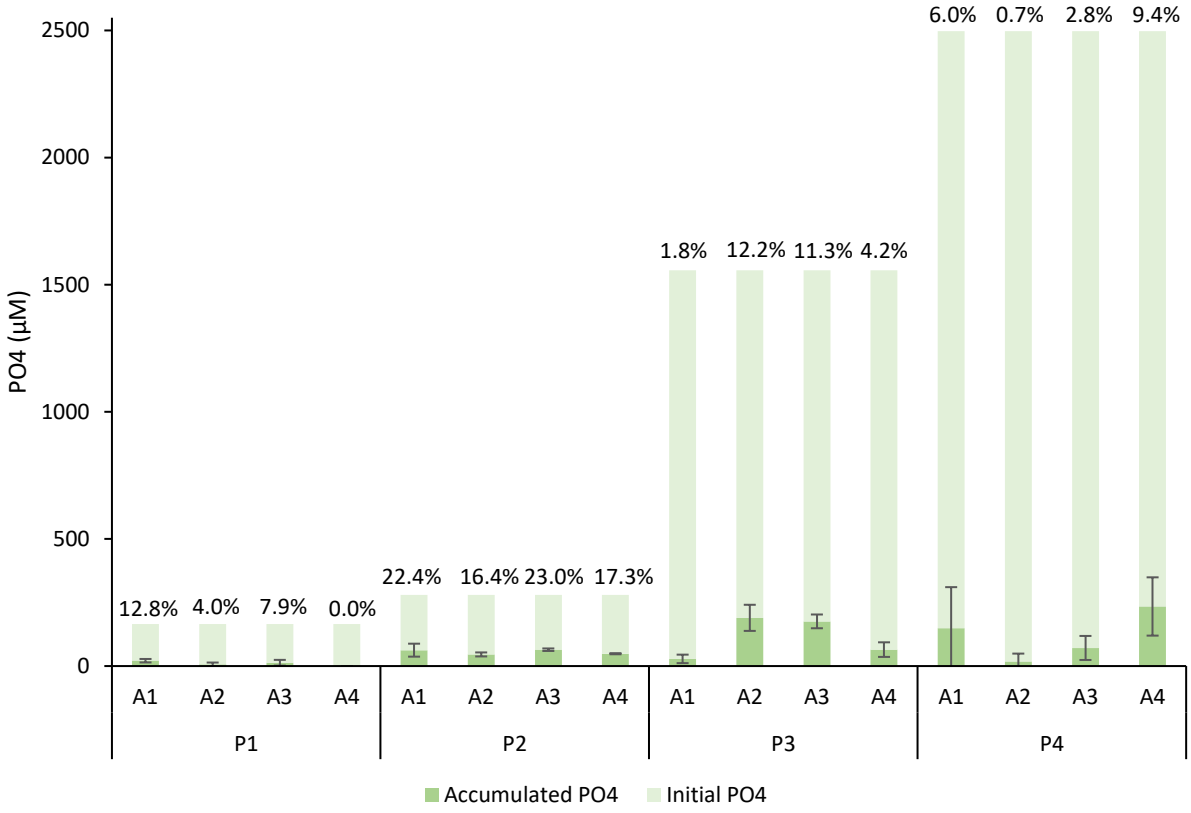

Figure 14: Phosphate accumulation of strain CL131 incubated in Syntho SWW for three days at 20°C. Light green columns indicate initial phosphate concentration while dark green columns indicate phosphate levels after incubation. P1-4 and A1-4 refer to different initial phosphate and acetate concentrations of the SWW. The percentage above the columns represents the proportion of initial phosphate accumulated by the bacterium. Values are represented as averages of triplicate measurements with standard deviation depicted as error bars.

On average, the phosphate uptake of strain CL131 was 10 ± 10 µM when incubated under P1 conditions, though that varied between acetate concentrations, as summarized in Figure 14. A1 resulted in the highest concentrations and A4 resulted in the lowest, on average. For P2 conditions, average uptake was 55 ± 14 µM. Some variation between the acetate concentrations was evident. The strain‘s average uptake when incubated under P3 conditions was 115 ± 78 µM, although deviation from that number can clearly be detected between the acetate conditions. The same applies to groups within P4, which collectively had an average

phosphate accumulation of 118 ± 122 µM. KW and DSCF showed that there was a significant statistical difference between some of the phosphate conditions, namely P1 and P2 ($p < 0.001$), P2 and P3 ($p < 0.001$) and P1 and P4 ($p = 0.022$).

The phosphate accumulation of CL188 differed between both phosphate and acetate concentrations, as seen in Figure 15.

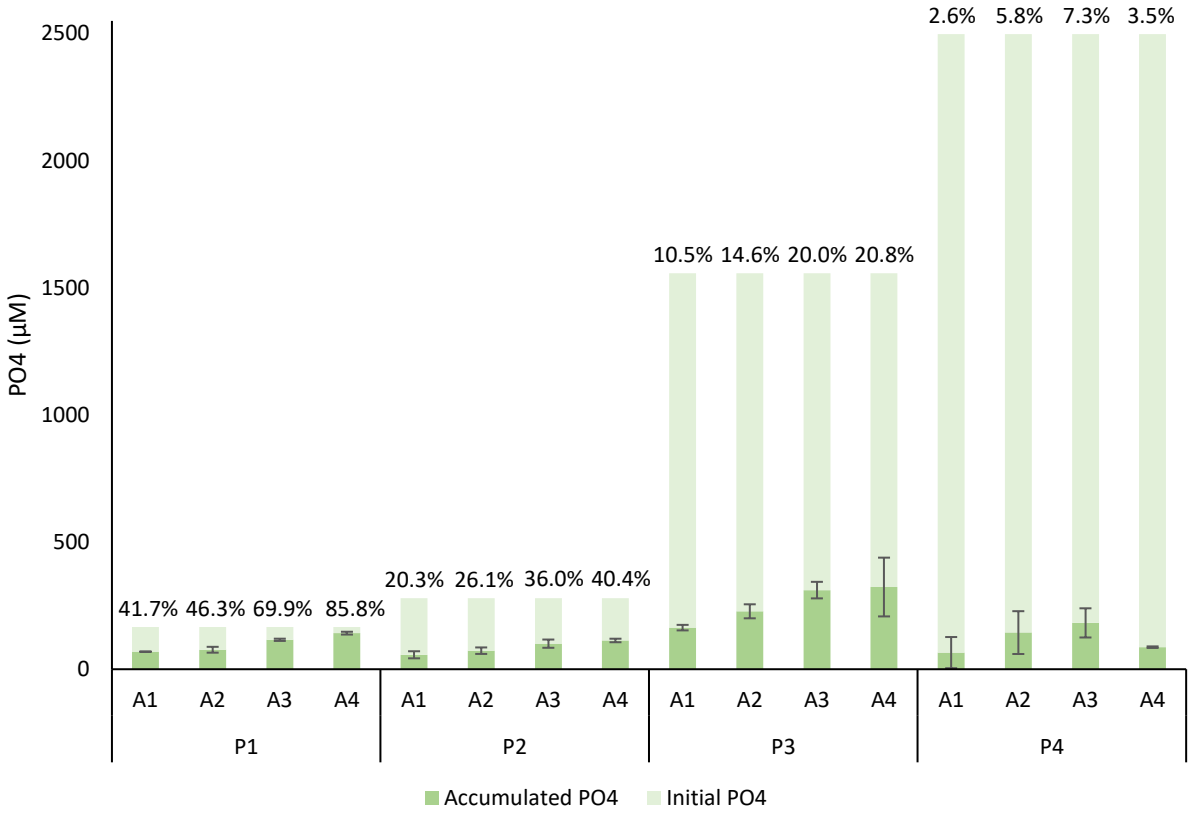

Figure 15: Phosphate accumulation of strain CL188 incubated in Syntho SWW for three days at 20°C. Light green columns indicate initial phosphate concentration while dark green columns indicate phosphate levels after incubation. P1-4 and A1-4 refer to different initial phosphate and acetate concentrations of the SWW. The percentage above the columns represents the proportion of initial phosphate accumulated by the bacterium. Values are represented as averages of triplicate measurements with standard deviation depicted as error bars.

The highest proportion of accumulated phosphate by CL188 was 85.8%, in P1A4, as seen in Figure 15. However, P3A4 conditions resulted in the highest amount of accumulated phosphate, which was on average 323.5 ± 115.6 µM. The phosphate uptake in P1 conditions was 101 ± 32 µM on average, though there was some variation between acetate concentrations, as applies for all of the phosphate groups. The lowest average phosphate accumulation occurred in P2 conditions, namely 86 ± 26 µM, while the highest average accumulation was seen in P3 conditions, as 257 ± 86 µM. For P4 conditions, average

phosphate uptake was 120 ± 70. KW and DSCF confirmed a significant difference between P3 and the three other phosphate groups, P1 ($p < 0.001$), P2 ($p < 0.001$) and P4 ($p = 0.005$). KW and DSCF also revealed a significant difference between groups incubated under A1 on one hand, and A3 on the other hand ($p = 0.046$).

In Figure 16, the aerobic phosphate accumulation results for CL197 are shown.

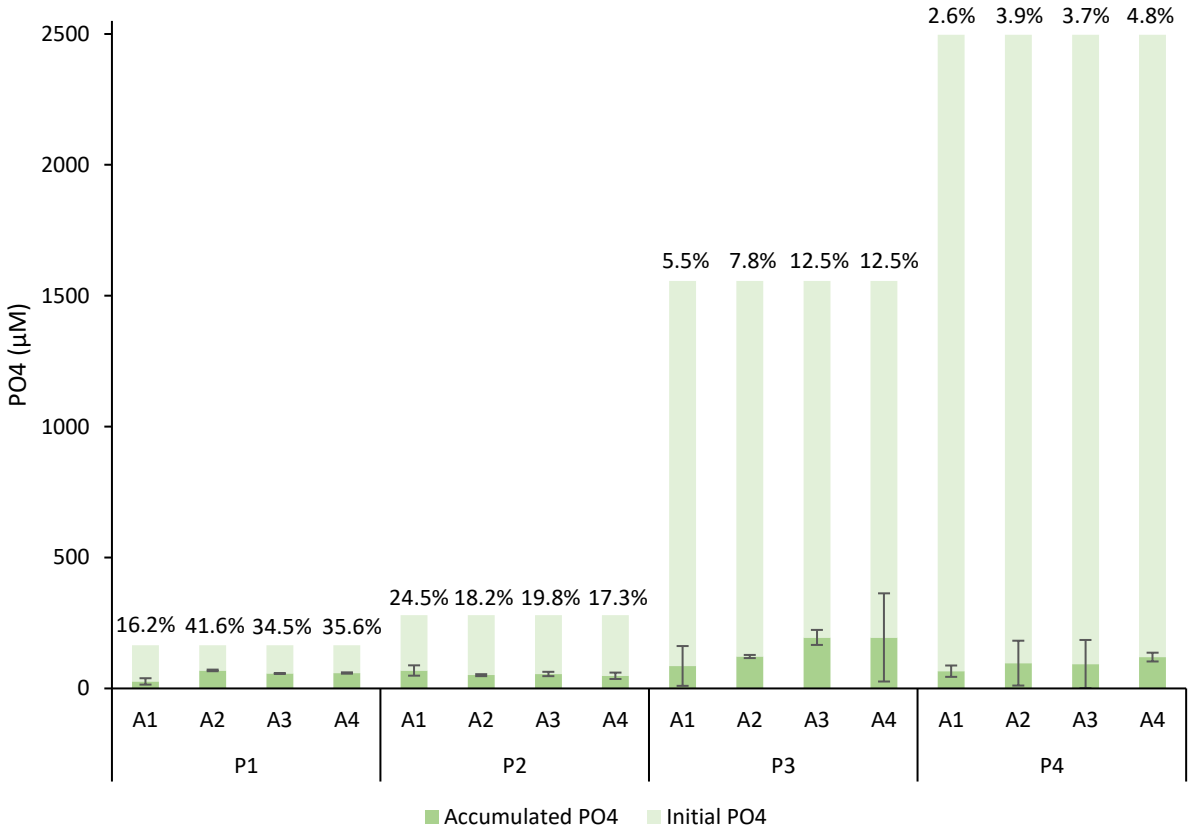

Figure 16: Phosphate accumulation of strain CL197 incubated in Syntho SWW for three days at 20°C. Light green columns indicate initial phosphate concentration while dark green columns indicate phosphate levels after incubation. P1-4 and A1-4 refer to different initial phosphate and acetate concentrations of the SWW. The percentage above the columns represents the proportion of initial phosphate accumulated by the bacterium. Values are represented as averages of triplicate measurements with standard deviation depicted as error bars.

The average phosphate uptake of groups within P1 was 53 ± 17 µM, which was similar to the groups within P2, being 56 ± 13 µM. As seen in Figure 16, the highest amounts of phosphorus were accumulated when the strain was incubated under P3A3 and P3A4 conditions, which both resulted in an average accumulation of 194.9 µM, although the standard deviation varied between those two groups. The average uptake of P3 groups collectively was 149 ± 94 µM. Incubation in P4 conditions resulted in 94 ± 58 µM accumulated

phosphate. KW and DSCF confirmed a significant difference between groups P1 and P3 (p = 0.003) and P2 and P3 (p = 0.003). No significant difference was detected between the acetate groups, when treated as four different groups, independent of initial phosphate concentrations.

The phosphate uptake of CL198 can be seen in Figure 17. The phosphate uptake varied between the phosphate conditions.

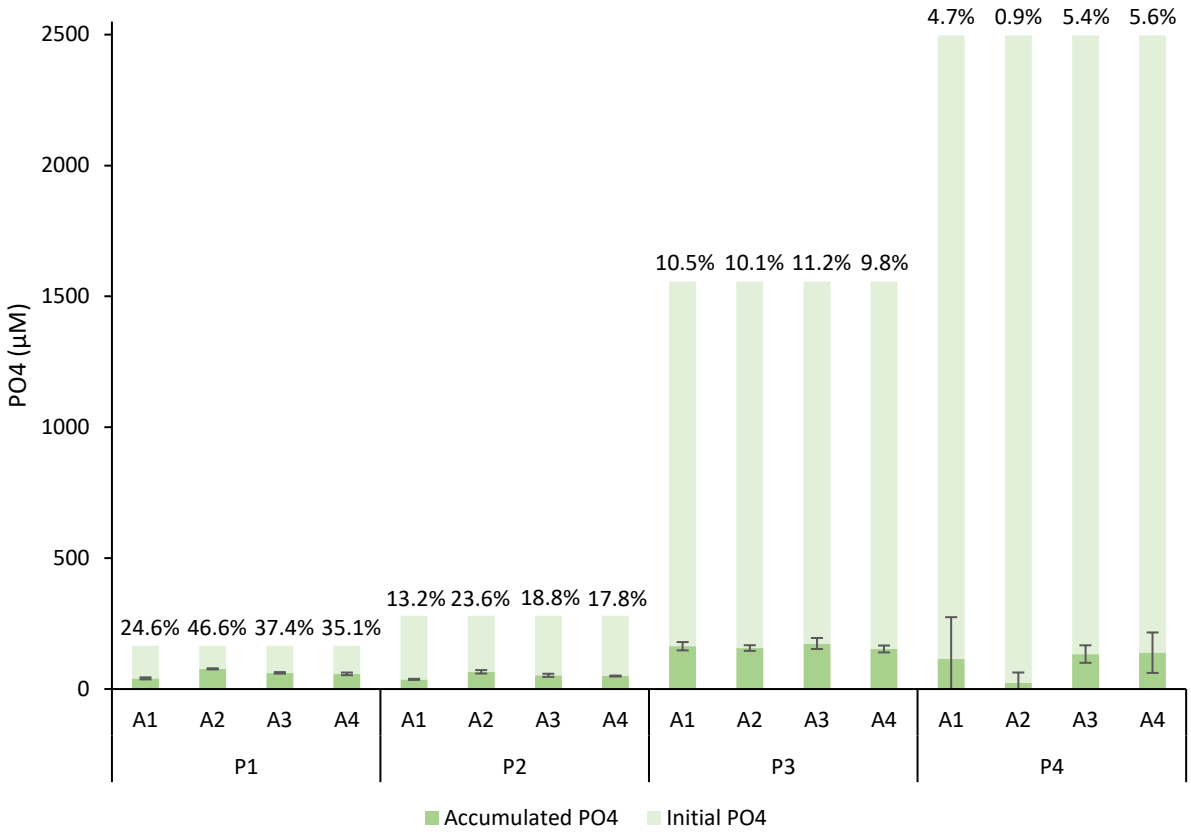

Figure 17: Phosphate accumulation of strain CL198 incubated in Syntho SWW for three days at 20°C. Light green columns indicate initial phosphate concentration while dark green columns indicate phosphate levels after incubation. P1-4 and A1-4 refer to different initial phosphate and acetate concentrations of the SWW. The percentage above the columns represents the proportion of initial phosphate accumulated by the bacterium. Values are represented as averages of triplicate measurements with standard deviation depicted as error bars.

As seen in Figure 17, the most phosphate was accumulated when the strain was incubated under P3 conditions. The uptake was 162 ± µM on average in P3. The lowest amount of phosphate was accumulated in P2 conditions, which was 51 ± 11 µM on average. The average accumulation in P1 was similar, or 59 ± 14 µM, while 103 ± 92 µM were accumulated on average in P4 groups. KW and DSCF showed that there was a statistically

significant difference between groups P1 and P3 ($p < 0.001$) and P2 and P3 ($p < 0.001$), but the difference in phosphate accumulation between acetate conditions was not significant.

The results for phosphate uptake by CL242 can be seen in Figure 18.

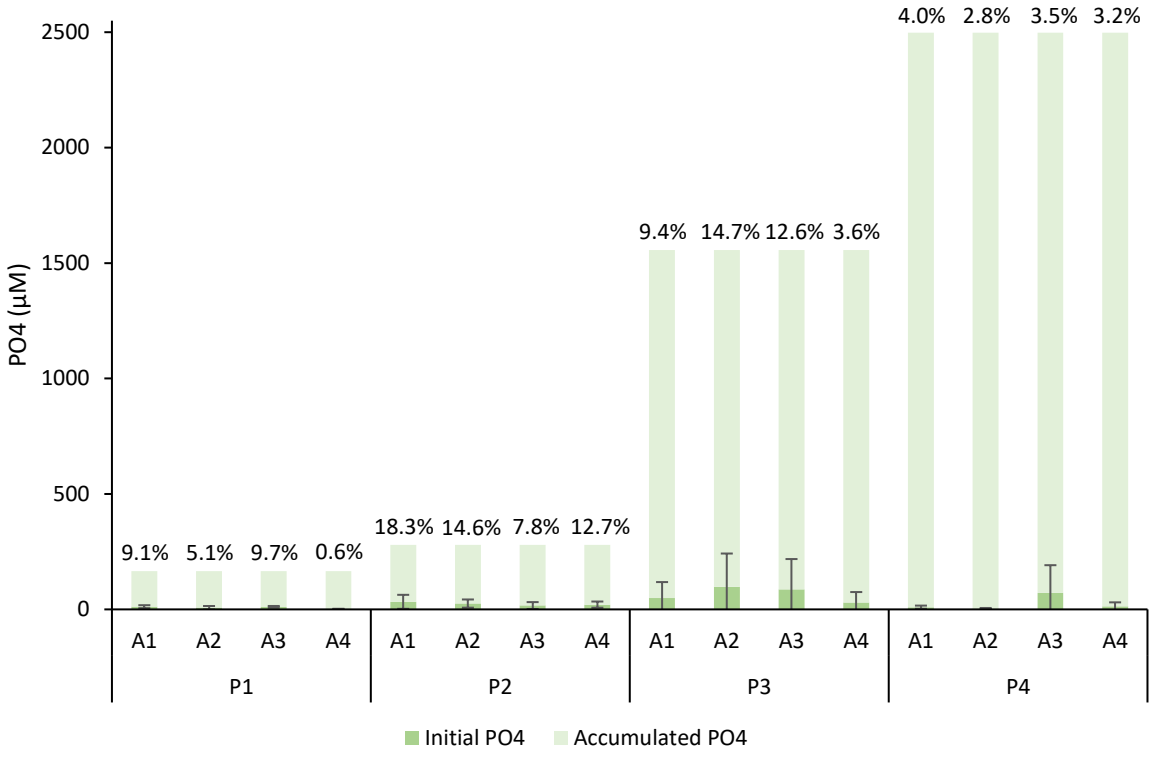

Figure 18: Phosphate accumulation of strain CL242 incubated in Syntho SWW for three days at 20°C. Light green columns indicate initial phosphate concentration while dark green columns indicate phosphate levels after incubation. P1-4 and A1-4 refer to different initial phosphate and acetate concentrations of the SWW. The percentage above the columns represents the proportion of initial phosphate accumulated by the bacterium. Values are represented as averages of triplicate measurements with standard deviation depicted as error bars.

As seen in Figure 18, the highest phosphate uptake occurred in P3 conditions, which was on average 66 ± 95 µM. The lowest average uptake was seen in group P1, which was 7.7 ± 6 µM. P4 groups had an average uptake of 24 ± 59 µM, similar to P1, whose average uptake was 24 ± 18 µM. KW and DSCF revealed a significant difference between P1 and P2 ($p < 0.001$), P1 and P3 ($p = 0.002$), P1 and P4 ($p = 0.005$) and P2 and P3 ($p = 0.003$).

3.2.3 OECD SWW: PHA production

The strains' PHA production when incubated in OECD SWW ranged from 0 to 885 µg/mL, as seen in Figure 19, where the results for each strain were put in a heatmap.

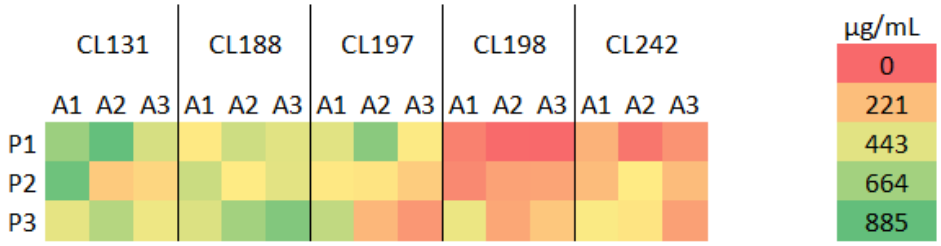

Figure 19: PHA produced by strains CL131, 188, 197, and 242 in OECD SWW after a three day incubation at 20°C. P1-3 and A1-3 refer to different initial phosphate and acetate concentrations of the SWW. Values are represented as averages of triplicate measurements. The lowest relative value is indicated by red and the highest relative value by green.

The PHA production varied between strains, as seen in Figure 19. On average, strain CL131 produced the most PHA of the five strains, when incubated under P1A2 conditions, with a measured amount of 885 µg/mL PHA. A similar amount, 848 µg/mL, was produced when the strain was incubated under P2A1 conditions. The strain's least PHA production was the result of incubation under P2A2 conditions, with 255 µg/mL PHA. For CL188, the highest PHA production was observed in P3A3 conditions with an average production of 778 µg/mL. The strain's lowest production was seen in P1A1 conditions, which was 335 µg/mL on average. Strain CL197 produced on average 751 µg/mL PHA when incubated in P1A2, while its lowest amount was the result of incubation under P3A3 conditions, at 122 µg/mL. Strain CL198 produced, on average, the lowest amount of PHA among the five strains. The highest amount of PHA was 408 µg/mL, detected in P3A1 wells, while the lowest amount was 0 µg/mL in P1A3. Lastly, strain CL242 produced the highest amount of PHA when incubated under P3A1 conditions, namely 358 µg/mL, and the lowest amount, 35 µg/mL, in P1A2 conditions.

As before, statistical tests were performed to assess the significance of the results. Due to small sample sizes, Kruskal-Wallis tests and subsequent DSCF post-hoc tests were performed on the data. The three groups of triplicates within each phosphate condition were treated as one group, and the same goes for the acetate groups. According to the KW, no statistically significant difference was present between either the phosphate groups or the acetate groups for strains CL131, CL188 and CL197. For CL198, there was a significant difference between groups P1 and P3 (p = 0.022) but no difference was detected between the acetate groups. KW

test detected a significant difference between some of the phosphate groups of CL242 (H (2) = 6.97, p = 0.031) but DSCF test failed to distinguish between which groups the difference existed.

3.2.4 Syntho SWW: PHA production

The results for the strains' PHA production was put in a heatmap, shown in Figure 20. The PHA production ranged from 0 to 569 µg/mL and varied between both acetate and phosphate concentrations.

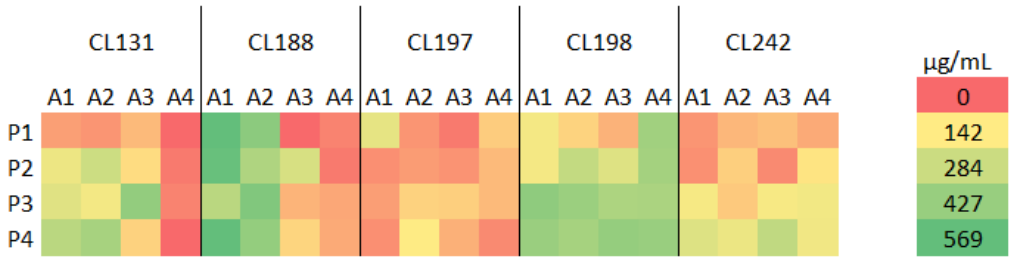

Figure 20: PHA produced by strains CL131, 188, 197, 198, and 242 in Syntho SWW after a three day incubation at 20°C. P1-4 and A1-4 refer to different initial phosphate and acetate concentrations of the SWW. Values are represented as averages of triplicate measurements. The lowest relative value is indicated by red and the highest relative value by green.

As seen in Figure 20, strain CL131 produced the least amount of PHA when incubated under A4 conditions, the production was close to or equal 0 µg/mL in all four cases. The strain produced the highest amount of PHA when incubated under P3A3 conditions, namely 439 µg/mL. Strain CL188 produced the highest amounts of PHA under A1 and A2 conditions, with the highest measurement of 569 µg/mL in both P1A1 and P4A1. This was the highest amount of PHA produced among the five strains in Syntho SWW. Incubation under A3 and A4 conditions resulted in 0 to 253 µg/mL. For CL197, the PHA production ranged from 20 to 212 µg/mL with no obvious trends for nutritional preferences. Strain CL198 produced the most PHA when incubated under P3 and P4 conditions, as well as A4 conditions, ranging from 367 to 450 µg/mL, while the lowest production was seen in P1A3 wells, namely 80 µg/mL. Strain CL242's PHA production ranged from 36 to 315 µg/mL, producing the highest amounts when incubated under P4 conditions and the lowest amounts under P1 and P2 conditions.

Statistical tests revealed a significant difference between some groups. KW and a subsequent DSCF for CL131 showed that there was a significant difference between P1 and P3 (p = 0.045), A1 and A4 (p = 0.004), A2 and A3 (p = 0.001) and A3 and A4 (p = 0.002). KW and DSCF for CL188 did not detect a significant difference between any phosphate groups, but

found a significant difference between groups A1 and A3 ($p = 0.007$), A1 and A4 ($p < 0.001$), A2 and A3 ($p = 0.003$) and A2 and A4 ($p < 0.001$). No significant difference was observed for groups within CL197, but for CL198, a significant difference was found between P1 and P3 ($p < 0.001$) and P2 and P3 ($p < 0.001$). Lastly, there was a significant difference between groups P1 and P2 ($p < 0.001$), P1 and P3 ($p = 0.002$), P1 and P4 ($p = 0.005$) and P2 and P3 ($p = 0.003$) for CL242.

3.3 Biochemical tests and characterization

Various biochemical and characterization tests were performed on the five strains. Results for the phosphate mobilization of the five selected strains are shown in Table 2. The results for the other strains can be seen in Table 15 in Appendix

Table 2: Phosphate mobilization results of strains CL131, 188, 197, 198, and 242. A positive test (halo formation) is indicated with "+" and a negative test (no halo formation) is indicated with "-". Growth without halo formation is indicated with G.

Media	NBRIP	NBRIP+NaCl	MAP
CL131	N/A	-	G
CL188	N/A	+	G
CL197	-	N/A	N/A
CL198	-	N/A	N/A
CL242	N/A	-	G

As can be seen in Table 2, no halo formation was evident on the MAP agar, but all strains could grow on the agar. Halo formation and thus phosphate solubilization was observed for one strain, CL188.

The results from Gram staining and KOH tests are shown on Table 3.

Table 3: Gram staining and KOH test results for strains CL131, 188, 197, 198, and 242. "-" and "+" indicate negative and positive tests, respectively.

Strain	Gram Result	Morphology	KOH result
CL131	-	Cocci, small cells	-
CL188	-	Cocci, small cells	-
CL197	-	Rods, big cells	-
CL198	-	Irregular cells	-
CL242	-	Rods, small cells	-

All the strains stained pink and so, the Gram staining was negative in all cases. The KOH tests were negatve as well, since no string formation was observed.

Results from biochemical tests and isolation media are shown in Table 4.

Table 4: Results from biochemical tests and selective isolation media for strains CL131, 188, 197, 198, and 242. A negative result is represented by "-", a weak positive result with "(+)" and a positive result with "+". For the selective media, "+" indicates a positive test (growth and color change) while G indicates just growth.

Test	CL131	CL188	CL197	CL198	CL242
H_2O_2	+	+	+	+	+
ARG	(+)	-	-	-	-
LYS	-	-	-	-	-
ORN	-	-	-	-	-
CIT	-	-	-	-	-
URE	-	+	-	-	-
MR	-	-	-	-	-
IND	-	-	-	-	-
VP	-	-	-	-	-
OF-F	(+)	(+)	+	+	(+)
OF-O	INC	(+)	+	+	(+)
NIT #1	-	-	-	-	+
NIT #2	-	-	-	-	N/A
EMB	-	-	-	-	-
MAC	-	-	-	-	-
Starch agar	-	G	G	G	-
MSA	-	+	+	+	-
BGA	-	G	G	G	-

As seen in Table 4, the OF-O test for CL131 was inconclusive, as the media developed a blue color after inoculation. All other tests were conclusive. All strains could – at least weakly – degrade glucose in the absence of oxygen. The NIT#1 results represent the color change after adding Nitrate Reduction Reagent to the inoculum (red color indicates a positive test), while

NIT#2 results represent the color change after adding zinc powder to the inoculum (red color indicates a negative test). All five strains were catalase positive.

In Table 5, results for the API strips are shown.

Table 5: API 20 E results for strains CL131, 188, 197, 198, and 242. A negative result is indicated with "-" and a positive test with "+".

Test	CL131	CL188	CL197	CL198	CL242
ONPG	-	-	-	-	-
ADH	-	-	-	-	-
LDC	-	-	-	-	-
ODC	-	-	-	-	-
CIT	-	-	-	-	-
H_2S	-	-	-	-	-
URE	-	-	-	-	-
TDA	-	-	-	-	-
IND	-	-	-	-	-
VP	-	-	-	-	-
GEL	-	-	+	+	-
GLU	-	-	-	-	-
MAN	-	-	-	-	-
INO	-	-	-	-	-
SOR	-	-	-	-	-
RHA	-	-	-	-	-
SAC	-	-	-	-	-
MEL	-	-	-	-	-
AMY	-	-	-	-	-
ARA	-	-	-	-	-

As evident on Table 5, all API strip test gave a negative result, except for the GEL tests of CL197 and CL198, which were positive.

Table 6 shows results from the temperature experiment.

Table 6: Temperature growth range of strains CL131, 188, 197, 198, and 242. "+" indicates good growth, "(+)" indicates weak growth and "-" indicates no growth.

Temperature (°C)	CL131	CL188	CL197	CL198	CL242
5	+	+	-	-	+
10	+	+	(+)	(+)	+
15	+	+	+	+	+
RT	+	+	+	+	+
30	+	+	+	+	+
35	-	-	+	+	-
50	-	-	-	-	-

As seen in Table 6, no strain grew at 50°C and all strains grew in temperatures ranging from 10°C to 30°C. CL197 and CL198 did not grow at 5°C, while the others did. Furthermore, they were the only strains that grew at 35°C.

3.4 DNA extraction and PCR

DNA extraction and 16S PCR was attempted for all five strains but was successful for three of them: CL131, CL197 and CL242. The gel on which the band from CL131 was visualized is seen in Figure 21 in Appendix and the gel on which the band from CL197 and CL242 were visualized are seen in Figure 22 in Appendix.

4 Discussion

The purpose of this study was to screen bacterial strains from the gut of *Arctica islandica* for the ability to accumulate phosphate and produce PHA from synthetic wastewater, as well as measuring their efficiency of doing so. Research on the microbiota of *Arctica islandica* remains underrepresented in the literature (Strahl & Abele, 2020), making this study an interesting contribution to the topic. The purpose was successfully achieved, as three strains from the CLAAM collection were identified in addition to the two strains that had been discovered during previous work, and measurements of their phosphate uptake and PHA production were carried out effectively. To answer the research questions, the promising PHA producing CLAAMs could remove phosphates from SWW under aerobic conditions, which is in accordance with the hypothesis. While a connection between the strains' phosphate removal and PHA production was observed, it was only in a binary manner, indicating that the only connection was that if the strains could produce PHA, they could accumulate phosphate. No relationship between the amounts of accumulated phosphate and PHA concentration was obvious, which is out of accord with the expected results.

4.1 Synthetic wastewater experiments

4.1.1 Phosphate accumulation

The phosphate accumulation observed herein varied between both the strains and the SWW's composition and ranged from 0 to 410 µM. The highest value corresponds to 38.9 mg/L phosphate or 12.7 mg/L phosphorus and an uptake rate of 36.2%. This was obtained by strain CL188 under P3A3 conditions in OECD SWW, as seen in Figure 10, where the initial phosphorus and acetate content was 35.1 mg/L and 86.4 mg/L respectively. However, this is a significantly higher amount of initial phosphate than what typical urban wastewater contains, which is often around 6-12 mg/L (Di Capua et al., 2022). In areas where wastewater is diluted (as is the case in Akureyri), the phosphorus content of wastewater reaches concentrations as low as 3.3 mg/L. Typically, the efficiency of biological aerobic phosphorus removal in WWTPs is around 20-30% (Di Capua et al., 2022), resulting in around 1-4 mg of phosphorus accumulated by the microbes per L. Therefore, the CLAAM strains compare positively to conventional WWTPs rates.

However, the data for phosphate accumulation under the P1 OECD SWW conditions, which are similar to the conditions of typical wastewater, containing 222.6 µM phosphate, corresponding to 6.9 mg/L phosphorus, suggests that the phosphate accumulation of the strains was similar to that of microbes in conventional WWTPs, with accumulation ranging from around 17 to 33%. This trend was not as obvious in the Syntho SWW, where conditions P1, containing 165.5 µM phosphate, corresponding to 5.1 mg phosphorus, and conditions P2, containing 279.7 µM phosphate, corresponding to 8.7 mg phosphorus. The uptake rates varied greatly between the strains, where CL188 showed the highest efficiency (85% in P1A4, as seen in Figure 15) and CL242 the lowest (0.6% in P1A4, as seen in Figure 18). Intriguingly, all the strains exhibited similar phosphate accumulation performances in the OECD SWW, while their performance in the Syntho SWW differed more. The effect of various acetate concentrations was also more evident in the Syntho SWW. It is worth noting that the uptake rate of CL188 was reasonably high when incubated under P1 conditions, especially when the acetate concentration was high. The uptake rate of 85.8%, approaches the effectiveness of EBPR systems (Di Capua et al., 2022). The initial phosphorus concentration was on the lower end of the conventional range, but still higher than that in Akureyri. This might be an interesting strain to further look at with relation to wastewater treatment in Iceland.

The effect of initial phosphate and acetate concentrations affected the strains differently depending on the type of SWW they were incubated in. In the OECD SWW, it seemed like the acetate concentration did not influence the strains' phosphate accumulation significantly. The phosphate concentration seems to have been the significant variable in the OECD in all cases. This was confirmed by statistical tests, which most often showed a significant relationship between initial phosphate concentration and phosphate uptake, but little effect of acetate concentration, even within groups that had the same phosphate concentrations. In the Synhto SWW, the acetate seemed to have more effect than was observed than in the OECD SWW, though this effect differed between strains. This was most obvious for strain CL188 (see Figure 15), where increasing acetate content resulted in increased phosphate uptake within each phosphate condition, although P4A4 was an exception to this trend. Interestingly, phosphate accumulation was higher in P1 on average than in P2 groups, but the accumulation in P3 was higher. This trend was also observed for strain CL198, as seen in Figure 17.

No relationship was observed between the C/P ratio of the SWWs and phosphate accumulation, which somewhat sits with previously discussed effect of acetate on the accumulation. The C/P ratios in the OECD SWW ranged from 0 to 13 (in P1A3, see Table 11), while the highest phosphate accumulation was seen in a C/P ratio of 2.6. The C/P ratios in the Syntho SWW ranged from 0 to 1427 (in P1A4, see Table 13) and the highest phosphate accumulation occurred under a C/P ratio of 125. Previously, it has been reported that C/P ratios ranging from 60 to 125 resulted in around 65.9% phosphorus removal efficiency in aerobic wastewater sludge, while the efficiency dropped to 40.1%, 30.2% and 23.0% with lower values of 50.0, 41.7 and 33.3, respectively (Chao et al., 2020). In addition, a novel PAO was found to accumulate phosphate effectively in conditions with C/P ratios in the range of 40 to 100 (Ni et al., 2021).

Each strain's phosphate accumulation performance in OECD SWW was compared to the same strain's performance in Syntho SWW. Generally, the strains accumulated similar or higher amounts of phosphate in OECD than in Syntho when the initial concentration was on the lower end (P1 OECD compared to P1 and P2 Syntho). The exception to this rule was strain CL188, which accumulated higher amounts of phosphate in the Syntho SWW in lower phosphate concentrations. When the initial phosphate concentration was higher (P3 OECD compared to P3 Syntho), all the strains accumulated higher amounts of phosphate in OECD than in Syntho.

From this it can be inferred that generally, the observed phosphate accumulation was enhanced by nutrient-low conditions coupled with higher initial phosphate concentrations (1134 µM).

Generally, the phosphate uptake seemed to increase with elevated initial phosphate concentration in the Syntho SWW, from P1 to P3, but then drop considerably when the strains were incubated under P4 conditions. This could be explained by limitations of the molybdenum blue method, discussed in section 4.4 below. Additionally, the high phosphate concentration might have inhibited the microbes' activity. While it has been reported that too high concentrations of phosphate in cytoplasm is toxic to cells (Bruna et al., 2021), little is known of how high phosphate concentrations in the environment affect bacterial growth directly, as phosphate is usually a limiting factor in ecosystems. However, De Bolle et al. (2013) showed that soil bacteria belonging to genera *Bacillus* and *Pseudomonas*, were able to grow in soils with high content of insoluble phosphate. Interestingly, inhibition of phosphate accumulation by acetate concentration was not observed, even though it was expected rather than phosphate inhibition as sodium acetate is a known food preservative (Sallam, 2007) and has been shown to inhibit the growth of various bacteria as well as eukaryotes such as yeast (Pinhal et al., 2019; Watcharawipas et al., 2018).

In relation to the discussion on phosphate uptake by bacteria, their minimum phosphorus requirement should be acknowledged. The knowledge of the minimum phosphorus requirement of bacterial cells is rather limited. According to reported data, minimum phosphorus content required by marine bacteria sampled from Raunefjorden in Norway was 2.3 fg phosphorus/cell (Vrede et al., 2002), corresponding to 0.16 mg phosphorus/L (given a cell density of 70 * 10^6 cells/L). Additionally, the phosphorus requirement of the nitrifying bacteria *Nitrobacter* and *Nitrosomonas* has been reported to be as low as 0.02 mg phosphorus/L (Meiklejohn, 1952). As mentioned before, the phosphate uptake by the CLAAMs corresponded to values ranging from 0 to 12.7 mg phosphorus/L. In the wells where phosphate accumulation measured 0, the bacteria would theoretically be dead, which they most likely were not if the PHA assay results can be trusted. This can most likely be attributed to shortcomings of the molybdenum blue method and more factors discussed in section 4.4. Other than that, the strains seemed to generally accumulate phosphorus in amounts higher than the minimum requirement, suggesting a surplus phosphorus accumulation.

4.1.2 PHA production

According to the PHA assay, all strains produced PHA, in various amounts. Currently, around 92 bacterial genera are known to have the ability to produce PHA, both aerobically and anaerobically, for example *Pseudomonas*, *Bacillus* and *Clostridium*. The polymer benefits the bacteria in more ways than solely as an energy source, as it can also be advantageous when exposed to stressful conditions such as freezing, osmotic pressure and oxidative pressure (Vicente et al., 2023). Based on this information, the CLAAM strains' ability to produce PHA might be an adaptation to the marine environment, as the ocean's salinity creates osmotic pressure that the bacteria must tolerate. Additionally, PHA reserves might be convenient to survive seasonal starvation phases, a common phenomenon in polar environments, like this one, induced by the nutrient-consuming growth of phytoplankton and thermal stratification in the summer (Valtýsson & Jónsson, 2000).

Out of all of the strains, CL131 produced the highest amount of PHA, 885 µg/mL, corresponding to 0.89 g/L, under P1A2 conditions in OECD SWW, where initial phosphate and acetate concentrations were 86.4 mg/L and 15.3 mg/L, respectively (see Figure 19). The strain produced a similar amount when incubated under P2A1 conditions, namely 848 µg/mL. The PHA production of the strain, along with CL188, was rather high compared to the other strains. One of the most studied PHA producing bacteria is *Cupriavidus necator*, also (syn. *Ralstonia eutropha*), has been reported to produce values as high as 15.28 g PHA/L (53% CDW), when incubated on molasses pretreated with sulphuric acid in a bioreactor, and a PHA content of up to 80% when incubated on date seed oil (6.2 g PHA/L) (Morlino et al., 2023). When *Cupriavidus necator* and strain CL131 are compared, it is clear that the CLAAM strain might not be ideal for PHA production.

Recently, incubating PHA producing species such as *Cupriavidus necator* in wastewater, as an affordable substrate for PHA production, has gained more interest. In a study by Khatami et al. (2022), PHA accumulation by the strain was up to 77% of cell dry weight when incubated in wastewater. PAOs in EBPR usually yield lower amounts of PHA as they decompose the polymer when taking up phosphate. For example, recent simultaneous PHA production and accumulation of phosphorus and nitrogen by PAOs in a novel configuration (SCEPPHAR) resulted in an average phosphorus recovery rate of 45% and PHA production in the range of 6.9 to 9.2% of the biomass (Larriba et al., 2020).

Both initial phosphate and acetate concentrations influenced the strains' PHA production in the two types of SWW, although a stronger effect was seen in Syntho. Moreover, this relationship affected the strains variously. Interestingly, some of the strains that were effective PHA producers in OECD were not as effective in Syntho, and vice versa. In the OECD SWW, CL131 seemed to prefer low phosphate (P1 and P2) and acetate (A1 and A2) conditions, while it seemed to be more effective in higher phosphate concentrations in Syntho. CL188 seemed to produce the highest PHA amounts in P3 conditions coupled with high acetate in OECD, while it seemed to prefer lower acetate concentrations, regardless of the phosphate concentration, in Syntho. CL197 produced more PHA in OECD, especially under low phosphorus conditions, than in Syntho, where it seemed to have no nutritional preference. On the other hand, CL198 was less effective in OECD, while having relatively high efficiency in Syntho, compared to the other strains, with preference for high phosphate concentration. The only strain that exhibited the same trend regarding nutrition in both SWW types was CL242, which did best under high phosphate concentrations.

As high C/P ratios have been reported to encourage PHA production, the highest amounts of PHA were expected in the P1 conditions coupled with high acetate concentrations. The highest C/P ratio in the OECD SWW was 13.1 in P1A3. This is low compared to previously reported values, which have ranged from 100 to 750, with the highest PHA production of 30.1% of cell dry weight when C/P ratio was 750 (Chao et al., 2020). In the Syntho SWW, the highest C/P ratio was 1247.2 in P1A4 conditions, a C/P ratio of 623.6 was seen in P2A4 and a ratio of 124.7 was seen in both P1A3 and P3A4 conditions. No relationship between the C/P ratios and PHA production was seen across the strains. Regardless, the effect of nitrogen limitation has been shown to have more effect than limitation by phosphorus (Wen et al., 2010), since the nitrogen content of the SWW was not measured or regulated, nothing can be deduced about the C/N ratio and its effects on the results.

The relationship between PHA production and phosphate accumulation is not obvious from the data. In the case of OECD SWW, PHA production in P2 conditions did not differ significantly from the other phosphate conditions, even though little to no phosphate accumulation was detected in P2. Additionally, though phosphate accumulation in P3 conditions was obviously higher than in all P1 groups, there was not a notable trend in the PHA production in relation to the phosphate content across the strains. Some of them produced the most PHA in P1, while

others were most effective in P3. In the case of Syntho SWW, the PHA production and phosphate accumulation did not seem to align either. For example, CL188 generally produced higher amounts of PHA under A1 and A2 conditions, regardless of initial phosphate content, but accumulated more phosphates under A3 and A4 conditions, in general. In addition, CL197 produced little PHA compared to the other strains, but had similar phosphate accumulation to CL198, which produced significantly higher amounts of PHA.

4.2 Ecological implications

Before 2020, all wastewater from Akureyri was released untreated into Eyjafjörður (Norðurorka, n.d.a), which could impact the clams' microbiota speciation and function. As mentioned before, the wastewater effluent from Akureyri contains on average 3.3 mg phosphorus/L, and while there are no regulations on how much phosphorus is allowed in wastewater effluents in Iceland, the European Union regulations limit the phosphorus discharge to 2 mg/L for towns with population equivalents under 100.000, as is the case in Akureyri (Commission directive 98/15/EC, 1998). It has previously been shown that pollution seems to affect the composition of the microbiota of Manila clams sampled in Venice lagoon in Italy. When exposed to higher levels of pollution, an increase in bacterial groups capable of metabolizing toxic chemicals was seen. In addition, a synergistic detoxifying action between the host and microbiota was observed when the clams were exposed to toxicants, suggesting that the microbiota might advantageously impact the clams' degradation of xenobiotics, increasing their resistance to chemicals in the environment (Milan et al., 2018). A similar effect might be expected in *Arctica islandica*, although the pollution in Eyjafjörður is thought to be lower than that in Venice lagoon, as the population of Venice is much larger than that of Akureyri. While the pollution is expected to be less in Eyjafjörður, it would be still be interesting and would provide valuable details about the ecology of the clams, to compare the CLAAM samples that were collected after 2020 with any known samples from before 2020.

Interestingly, both the highest amount of PHA produced, and the highest amount of phosphate accumulated, occurred in the OECD SWW, which was nutrient-poor. This is somewhat unsurprising as microbial PHA production tends to be positively influenced by nutrient limitation, such as nitrogen and phosphorus (Wen et al., 2010). However, this might also be explained by the fact that the organisms are adapted to the nutrient-poor conditions in

their natural environment, the gut of clams. This leads to speculations on the role of the bacteria in the clams. As mentioned in the introduction, it has been shown that the gut microbiota is a crucial part of the clams' function. The gut microbiota may play a role as nutrient accumulators, helping the clams to obtain essential nutrients for their growth and maintenance.

4.3 Characterization

All of the strains got a negative result from the KOH tests, which implies that they are Gram positive (see Table 3). The results from the Gram staining, however, indicated that the strains were Gram negative. Although Gram staining is a widely used technique in diagnostic testing of microbes, it is considered a high-complexity method, increasing the risk of error. Factors such as reader error and smear preparation can impact the results. If the cellular content on the slides is too high, it can lead to overly thick smears which increases the risk of false-negative results (Samuel et al., 2016). This is a plausible explanation to the inagreement between these two tests. The results from the PCR and electrophoresis further support this hypothesis, as samples containing extracted DNA gave rise to bands on the gel in some cases (3 out of 5 strains), while untreated material from the same strains did not show any bands (see Figure 21 and Figure 22). This may further support the conclusion of erroneous Gram staining, as it has been reported that the thick cell wall of gram positive bacteria is more resistant to heat lysis during the PCR, resulting in less effective DNA extraction and less PCR product yield. When mechanical disruption method like beat-beating was used, the DNA extraction of Gram positive bacteria was more effective (Kai et al., 2019).

Regarding the biochemical tests (see Table 4), all strains gave a positive catalase test (H_2O_2), which means they produce the enzyme catalase, responsible for neutralization of hydrogen peroxide. This is a common ability amongst aerobic bacteria as hydrogen peroxide is formed during aerobic metabolic processes but causes oxidative stress. Thus, it can be deduced that the CLAAM strains are most likely aerobic or facultatively aerobic, which is not surprising considering their natural environment (Yuan et al., 2021). The only strain able to hydrolyse arginine was CL131, which did so only weakly, suggesting it posesses the enzyme arginine dihydrolase. In the process of the hydrolysis, ammonium is formed as a side product, which has been correlated to the protection of bacteria in acidic environment as it lowers the pH (Novák

et al., 2016). Strain CL188 was able to break down urea suggesting the presence of a urease, an enzyme that catalyses the hydrolysis of urea. It has been shown that urease-producers may play an important role in the marine nitrogen cycle, by supplying primary producers with inorganic nitrogen, which is formed in this process (Pei et al., 2024).

Additionally, all strains were able to degrade glucose under both aerobic (excluding CL131, inconclusive results) and anaerobic conditions indicating they are facultative anaerobes. The only strain able to reduce nitrate to nitrite was CL242. All the API strip tests gave a negative result, excluding the GEL test of CL197 and CL198, as seen in Table 16, indicating that they possess the enzyme gelatinase (BioMérieux, n.d.). Only one strain was able to mobilize phosphate from the NBRIP agar, namely CL188. The enzymes responsible for the mobilization of phosphate, collectively named phosphatases, are not the same as the enzymes utilized in the accumulation of phosphates, so it is to no surprise that the other strains did not give a positive results in this assay. Phosphate mobilizing bacteria are important in the cycling of phosphorus in soils, and are thought to play a role in the marine phosphorus cycle as well (Saranya et al., 2022), which might apply to CL188.

None of the strains were able to grow on EMB agar (see Table 4), which is selective for Gram negative bacteria, as the agar contains Eosin Y, which is toxic to Gram positive bacteria. This further indicates that all strains are Gram positive, supporting the assumptions made from the KOH results. No growth was observed on the MAC plates, indicating that the strains are all Gram positive. Three strains, CL188, CL197 and CL198, gave a positive result on the MSA agar, suggesting that they belong to the genera *Staphylococcus* or *Micrococcus*. The morphology of CL188 observed after Gram staining agrees with this result, as the cells appeared spherical. However, the cells of CL197 were shaped like rods and the shape of CL98 could not be determined due to bad sample quality. As discussed earlier, the Gram staining is not considered as reliable as the isolation media. The possibility of the strains belonging to the genus *Salmonella* can be ruled out, as none of them gave a positive result on the BGA media. No strain showed the ability to hydrolyse starch (Zimbro et al., 2009).

Interestingly, strains CL197 and CL198 gave the same results in most of the biochemical tests and isolation media. Additionally, their colonies looked the same and their temperature growth range was identical. In fact, they were the only two strains that could not grow at 5°C, and the only ones that could grow at 35°C (see Table 6). The other strains grew in the range of

5 to 30°C. The fact that the strains could not grow at 5°C is interesting in itself, as the annual average temperature of the sea in Eyjafjörður is around 4 to 5°C. The temperature frequently gets lower than that, with an average of 1°C in the coldest periods (Valtýsson & Jónsson, 2000). A possible explanation to this matter is that the strains might be able to survive at these low temperatures in the coexistence of the gut microbial community. The two strains‘ phosphate accumulation followed a similar pattern and when stained with Sudan Black, they both seemed to contain intracellular granules that stained more intensely than the rest of the colonies (see Figure 8). These are thought to be polymeric reserves of fatty substances, possibly PHA. Based on this, it is hypothezised that CL197 and CL198 are the same strain, which happened to be isolated twice. However, the two strains did not look the same in Gram staining, and produced various amounts of PHA under the same conditions, which counts against the aforementioned hypothesis.

4.4 Research limitations and future directions

The method used in this current work for the screening of potential PHA producers, and consequently potential phosphate accumulators, has its drawbacks. Although Sudan Black has been widely used as a presumptive test for PHA production, it binds to various kinds of intracellular fats and lipophilic substances (Serafim et al., 2002). This might have impacted the screening results, with the possibility of false positive tests, although that did not seem to be the case for the selected strains, as PHA was measured in all of them. However, as the same reagent was used in the PHA assay, this limitation also applies to that method, increasing the risk of measuring higher amount of PHA than was present. The Toluidine blue O (TBO) agar assay might represent a more reliable and accurate method for PAO screening. The method utilizes an agar supplemented with TBO, which forms a colored complex with phosphate and gets incorporated into the colonies as they grow. The cells‘ phosphate accumulation can then be evaluated based on the intensity of the colonies‘ color, which corresponds to the concentration of intracellularly stored phosphate. However, it has been shown that this method has limited sensitivity, reliability and specificity (Anand & Aoyagi, 2019a; Anand & Aoyagi, 2019b).

Yet another method to identify PAOs is to target the genes responsible for their behavior, such as phosphate uptake and polyphosphate synthesis. As mentioned before, knowledge on the PAOs' key genes remains limited, though a dysregulation in the Pho regulon of *Ca.* Accumulibacter is thought to cause ineffective regulation of *pst*, which in turn is thought to lead to excessive phosphate uptake. The genome of *Ca.* Accumulibacter, which is a model PAO, is well known, while the genomes of other PAOs need more research (Xie et al., 2024). The Pho regulon is a prevalent phosphorus regulatory system in bacteria, some parts of it are better conserved than others, making advantageous primer binding sites for sequencing (Monds et al., 2006).

Another issue worth noting is that measurements of the initial phosphate content in both types of SWW suggested higher concentrations than what can be attributed to the phosphate-containing chemicals added to the media. The difference between the calculated initial phosphate value and the measured initial phosphate value was various between the phosphate levels, the lowest difference observed in the P1 groups, where the difference was 61 µM, corresponding to 28% in OECD and 48 µM, corresponding to 29% in Syntho, and the highest difference was observed in the P3 groups, where the difference was 331 µM, corresponding to 29% in OECD, and 384 µM, corresponding to 25% in Syntho. Interestingly, the proportional difference was around 28 to 29% in all three cases in the OECD SWW, but ranged from 6 to 29% in the Syntho SWW. Since this difference varied between conditions, it did not only stem from a source in some components of the media that had not been taken into account in the calculations. It is hypothesized that the phosphate interacted differently with components in the media, depending on its concentration The acetate concentration did not seem to have profound effect, therefore interaction with other components is suspected. Additionally, it is possible that the phosphate assay had some limitations causing this effect, as mentioned before (Anand & Aoyagi, 2019a).

If a look is taken on the accumulation values and uptake rates for the five strains incubated in OECD, a prominent trend can be seen, which is that the P2 condition had by far the lowest uptake rates, while P1 and P3 uptake rates typically ranged from approximately 20 to 30% (as is typical for aerobic P-uptake). A possible explanation for this is that the phosphate assay (molybdenum blue method or ascorbic acid method) might be subjected to error. When measuring the phosphate, it was necessary to dilute the samples obtained from conditions P2

and P3 by 1/10, since the standard curve‘s upper limits were 50 µM phosphate. More concentrated standards did not yield a linear reading. All samples were measured both undiluted and after a 1/10 dilution. The results varied significantly between the two measurements for each sample, as the diluted samples resulted in a much lower number, typically 50-60% with an average of 55% (this applies to the values obtained from the standard curves, before further calculations to take into account the dilutions and initial phosphate content). It was decided to use the results from undiluted measurements for P1, as they fit the standard curve, but the P2 and P3 samples fell beyond the standard curve when undiluted. This led to much higher values in P1 compared to P2 and P3.

It has been reported that the molybdenum blue method is limited by the presence of antimony in potassium antimony tartrate, which is used as a reagent. Higher antimony concentrations cause an increase in turbidity and decrease dependability. Other limiting factors include the sample‘s ionic strength, acid concentration and presence of persulfates (Anand & Aoyagi, 2019a). In the case of ionic strength, higher amounts of ions from compounds such as NaCl causes phosphate particles to settle out increasing turbidity, which in turn increases the light absorbance of the sample. This effect has been seen to increase with higher phosphate contents (De Haas et al., 1990).

The reliability of the results can be questioned, as the RSD was often over 15%, which is considered the acceptable limits in microbial experiments (Zhao, L. et al., 2017). This applies to both phosphate accumulation results as well as PHA production. In extreme cases, the RSD values got as high as 170%, which shows how much deviation was present in the data, diminishing its reliability.

According to the literature, EBPR assumes an anaerobic step followed by an aerobic step to optimize phosphate uptake. In this experiment, the strains were only incubated under aerobic conditions as successful PHA production has previously been achieved under aerobic conditions using strains from the CLAAM collection. Anaerobic conditions are yet to be explored for this set of organisms. This might have significantly impacted the results for both PHA production and phosphate uptake. A typical behvior by PAOs is production of PHA at high C/P ratios, while phosphate is accumulated at low C/P ratios (Korkakaki et al., 2017). No such relationship was obvious in the data. Continuing research would be needed to study the strains‘ performance in anaerobic conditions or EBPR, as well as various environmental conditions such

as pH and salinity, to determine their utility further. Additionally, sequencing the strains would give valuable information, both regarding the wastewater aspects, but also on the ecological side. The sequencing has already been prepared and the PCR products are stored in the freezer, waiting to be sent to the Netherlands.

5 Conclusions

The ability of five strains isolated from clam guts to accumulate phosphate from synthetic wastewater and subsequently produce intracellular PHA was investigated. A presumptive Sudan Black staining was used as a screening method to identify potential PHA producers, and consequently possible phosphate accumulators. Two types of SWW were used (nutrient-rich and nutrient-poor), containing various initial amounts of phosphate and acetate. All strains produced PHA to some extent. The highest amount, 38.9 mg/L, was produced by CL188 in nutrient-poor SWW initially containing 5.0 mg/L phosphate and 86.4 mg/L acetate. This amount is low in comparison to the well-known PHA producer *Cupriavidus necator*, which has been reported to produce up to 15.28 g PHA/L (under optimum conditions), although PAOs normally synthesise lower amounts of PHA. The strains' ability to accumulate phosphate under conditions typical for wastewater (nutrient-poor containing 15.3 mg /L phosphate), was similar to that of activated sludge in WWTPs, with uptake rates of 17-30%. Interestingly, CL188 accumulated 85% of the phosphate when incubated in nutrient-rich SWW containing 8.6 g/L acetate and 15.6 mgL phosphate, which is similar to the efficiency of EBPR, although the acetate concentration is higher than in real-life situations. That said, lower initial acetate concentrations also resulted in high phosphate accumulation. Although the PHA assay results were not propitious, the phosphate accumulation, especially that of CL188 and CL131, gave promising results that warrant further investigation. This would include setting up EBPR system to see how the strains would behave in conditions optimised for phosphate accumulation, as well as various ranges of pH, salinity and temperature. The screening of the collection could also be repeated with improved methodology, targeting PAO genes or phosphate accumulation abilities directly with TBO agar assay.

References

Achbergerova, L., & Nahalka, J. (2011). Polyphosphate - an ancient energy source and active metabolic regulator. *Microbial Cell Factories, 10*(63), 63. https://doi.org/10.1186/1475-2859-10-63

Alewell, C., Ringeval, B., Ballabio, C., Robinson, D. A., Panagos, P., & Borrelli, P. (2020). Global phosphorus shortage will be aggravated by soil erosion. *Nature Communications, 11*(1), 4546. https://doi.org/10.1038/s41467-020-18326-7

Anand, A., & Aoyagi, H. (2019a). Estimation of microbial phosphate-accumulation abilities. *Scientific Reports, 9*(1), 4879. https://doi.org/10.1038/s41598-018-37752-8

Anand, A., & Aoyagi, H. (2019b). A high throughput isolation method for phosphate-accumulating organisms. *Scientific Reports, 9*(1), 18083. https://doi.org/10.1038/s41598-019-53429-2

Bindraban, P. S., Dimkpa, C. O., & Pandey, R. (2020). Exploring phosphorus fertilizers and fertilization strategies for improved human and environmental health. *Biology and Fertility of Soils, 56*(3), 299-317. https://doi.org/10.1007/s00374-019-01430-2

BioMérieux. (n.d.). *API 20 E.* https://biomanufacturing.org/uploads/files/587872707301898351-api20einstructions.pdf

Boeije, G., Corstanje, R., Rottiers, A., & Schowanek, D. (1999). Adaptation of the CAS test system and synthetic sewage for biological nutrient removal: Part I: Development of a new synthetic sewage. *Chemosphere (Oxford), 38*(4), 699-709. https://doi.org/10.1016/S0045-6535(98)00311-7

Bruna, R. E., Kendra, C. G., Groisman, E. A., & Pontes, M. H. (2021). Limitation of phosphate assimilation maintains cytoplasmic magnesium homeostasis. *Proceedings of the National Academy of Sciences - PNAS, 118*(11), e2021370118. https://doi.org/10.1073/pnas.2021370118

Cakmak, E. K., Hartl, M., Kisser, J., & Cetecioglu, Z. (2022). Phosphorus mining from eutrophic marine environment towards a blue economy: The role of bio-based applications. *Water Research (Oxford), 219*, 118505. https://doi.org/10.1016/j.watres.2022.118505

Chao, C., Zhao, Y., Keskar, J., Ji, M., Wang, Z., & Li, X. (2020). Simultaneous removal of COD, nitrogen and phosphorus and the tridimensional microbial response in a sequencing batch biofilm reactor: With varying C/N/P ratios. *Biochemical Engineering Journal, 154*, 107215. https://doi.org/10.1016/j.bej.2019.04.017

Chrispim, M. C., Scholz, M., & Nolasco, M. A. (2019). Phosphorus recovery from municipal wastewater treatment: Critical review of challenges and opportunities for developing countries. *Journal of Environmental Management, 248*, 109268. https://doi.org/10.1016/j.jenvman.2019.109268

Commission directive 98/15/EC, (1998). https://eur-lex.europa.eu/legal-content/EN/TXT/?uri=CELEX%3A01998L0015-19980327

Cordell, D., & White, S. (2015). Tracking phosphorus security: Indicators of phosphorus vulnerability in the global food system. *Food Security, 7*(2), 337-350. https://doi.org/10.1007/s12571-015-0442-0

Crini, G., & Lichtfouse, E. (2018). Wastewater treatment: An overview. In E. Lichtfouse, & G. Crini (Eds.), *Green adsorbents for pollutant removal : Fundamentals and design* (1st ed., pp. 1-21). Springer International Publishing. https://doi.org/https://doi.org/10.1007/978-3-319-92111-2_1

D'costa, A. H., S.K., S., M.K., P. K., & Furtado, S. (2018). The backwater clam (meretrix casta) as a bioindicator species for monitoring the pollution of an estuarine environment by genotoxic agents. *Mutation Research. Genetic Toxicology and Environmental Mutagenesis, 825*, 8-14. https://doi.org/10.1016/j.mrgentox.2017.11.001

Dai, W., Dong, Y., Ye, J., Xue, Q., & Lin, Z. (2022). Gut microbiome composition likely affects the growth of razor clam sinonovacula constricta. *Aquaculture, 550*, 737847. https://doi.org/10.1016/j.aquaculture.2021.737847

De Bolle, S., Gebremikael, M. T., Maervoet, V., & De Neve, S. (2013). Performance of phosphate-solubilizing bacteria in soil under high phosphorus conditions. *Biology and Fertility of Soils, 49*(6), 705-714. https://doi.org/10.1007/s00374-012-0759-1

De Haas, D. W., Lotter, L. H., & Dubery, I. A. (1990). An evaluation of the methods used for the determination of orthophosphate and total phosphate in activated sludge extracts. *Water S. A., 16*(1), 55-65. http://hdl.handle.net/10520/AJA03784738_1757

Di Capua, F., de Sario, S., Ferraro, A., Petrella, A., Race, M., Pirozzi, F., Fratino, U., & Spasiano, D. (2022). Phosphorous removal and recovery from urban wastewater: Current practices and new directions. *The Science of the Total Environment, 823*, 153750. https://doi.org/10.1016/j.scitotenv.2022.153750

Ding, J., Sun, C., He, C., Li, J., Ju, P., & Li, F. (2021). Microplastics in four bivalve species and basis for using bivalves as bioindicators of microplastic pollution. *The Science of the Total Environment, 782*, 146830. https://doi.org/10.1016/j.scitotenv.2021.146830

Dorofeev, A. G., Nikolaev, Y. A., Mardanov, A. V., & Pimenov, N. V. (2020). Role of phosphate-accumulating bacteria in biological phosphorus removal from wastewater. *Applied Biochemistry and Microbiology, 56*(1), 1-14. https://doi.org/10.1134/S0003683820010056

Duperron, S., Gaudron, S. M., Rodrigues, C. F., Cunha, M. R., Decker, C., & Olu, K. (2013). An overview of chemosynthetic symbioses in bivalves from the north atlantic and mediterranean sea. *Biogeosciences, 10*(5), 3241-3267. https://doi.org/10.5194/bg-10-3241-2013

Eniafe, J., & Jiang, S. (2021). The functional roles of TCA cycle metabolites in cancer. *Oncogene, 40*(19), 3351-3363. https://doi.org/10.1038/s41388-020-01639-8

European Commission. (2022, Feb 9,). *Urban waste water: Commission decides to refer POLAND to the court of justice of the european union for lack of treatment of its waste waters* [Press release]. https://ec.europa.eu/commission/presscorner/detail/en/ip_22_582

European Commission. (2023, Dec 21,). *Water: Commission refers SPAIN to the court of justice for its failure to comply with the urban waste water treatment directive* [Press release]. https://ec.europa.eu/commission/presscorner/detail/en/ip_23_6343

European Commission. (2024, Mar 13,). *The commission decides to refer ITALY to the court of justice of the european union for failure to fully comply with the urban wastewater treatment directive* [Press release]. https://ec.europa.eu/commission/presscorner/detail/en/ip_24_1234

Gedda, G., Balakrishn, K., Uma, R., & Shah, K. J. (2021). Introduction to conventional wastewater treatment technologies: Limitations and recent advances. In Vimal Gandhi, & Kinjal Shah (Eds.), *Advances in wastewater treatment I* (pp. 1-36). Materials Research Forum LLC.

Genesis Water Tech. (2023, August 23,). *Primary treatment methods for suspended solids in wastewater.* https://genesiswatertech.com/. Retrieved March 23, 2024, from https://genesiswatertech.com/blog-post/primary-treatment-methods-for-suspended-solids-in-wastewater/

Gunnarsdóttir, R., Jenssen, P. D., Erland Jensen, P., Villumsen, A., & Kallenborn, R. (2013). A review of wastewater handling in the arctic with special reference to pharmaceuticals and personal care products (PPCPs) and microbial pollution. *Ecological Engineering, 50*, 76-85. https://doi.org/10.1016/j.ecoleng.2012.04.025

Havukainen, J., Nguyen, M. T., Hermann, L., Horttanainen, M., Mikkilä, M., Deviatkin, I., & Linnanen, L. (2016). Potential of phosphorus recovery from sewage sludge and manure ash by thermochemical treatment. *Waste Management (Elmsford), 49*, 221-229. https://doi.org/10.1016/j.wasman.2016.01.020

Huang, M., Li, Y., & Gu, G. (2010). Chemical composition of organic matters in domestic wastewater. *Desalination, 262*(1), 36-42. https://doi.org/10.1016/j.desal.2010.05.037

Ingólfur Bender, Margrét Kristín Sigurðardóttir, & Sigurður Hannesson. (2021). *Innviðir á íslandi 2021- ástand og framtíðarhorfur.* Samtök iðnaðarins. https://www.si.is/media/_eplica-uppsetning/Innvidir-a-Islandi_skyrsla_opnur.pdf

Izadi, P., Izadi, P., & Eldyasti, A. (2020). Design, operation and technology configurations for enhanced biological phosphorus removal (EBPR) process: A review. *Reviews in Environmental Science and Biotechnology, 19*(3), 561-593. https://doi.org/10.1007/s11157-020-09538-w

Jones, E. R., van Vliet, M. T. H., Qadir, M., & Bierkens, M. F. P. (2021). Country-level and gridded estimates of wastewater production, collection, treatment and reuse. *Earth System Science Data, 13*(2), 237-254. https://doi.org/10.5194/essd-13-237-2021

Kai, S., Matsuo, Y., Nakagawa, S., Kryukov, K., Matsukawa, S., Tanaka, H., Iwai, T., Imanishi, T., & Hirota, K. (2019). Rapid bacterial identification by direct PCR amplification of 16S rRNA genes using the MinION™ nanopore sequencer. *FEBS Open Bio, 9*(3), 548-557. https://doi.org/10.1002/2211-5463.12590

Kesari, K. K., Soni, R., Jamal, Q. M. S., Tripathi, P., Lal, J. A., Jha, N. K., Siddiqui, M. H., Kumar, P., Tripathi, V., & Ruokolainen, J. (2021). Wastewater treatment and reuse: A review of its applications and health implications. *Water, Air, and Soil Pollution, 232*(5), 208. https://doi.org/10.1007/s11270-021-05154-8

Khan, S., & Ali, J. (2018). 2 - chemical analysis of air and water. In Donat-P. Häder, & Gilmar S. Erzinger (Eds.), *Bioassays* (pp. 21-39). Elsevier Inc. https://doi.org/10.1016/B978-0-12-811861-0.00002-4

Khatami, K., Perez-Zabaleta, M., & Cetecioglu, Z. (2022). Pure cultures for synthetic culture development: Next level municipal waste treatment for polyhydroxyalkanoates production. *Journal of Environmental Management, 305*, 114337. https://doi.org/10.1016/j.jenvman.2021.114337

Korkakaki, E., van Loosdrecht, M. C. M., & Kleerebezem, R. (2017). Impact of phosphate limitation on PHA production in a feast-famine process. *Water Research (Oxford), 126*, 472-480. https://doi.org/10.1016/j.watres.2017.09.031

Lambers, H. (2022). Phosphorus acquisition and utilization in plants. *Annual Review of Plant Biology, 73*(1), 17-42. https://doi.org/10.1146/annurev-arplant-102720-125738

Larriba, O., Rovira-Cal, E., Juznic-Zonta, Z., Guisasola, A., & Baeza, J. A. (2020). Evaluation of the integration of P recovery, polyhydroxyalkanoate production and short cut nitrogen removal in a mainstream wastewater treatment process. *Water Research (Oxford), 172*, 115474. https://doi.org/10.1016/j.watres.2020.115474

Li, Y., Hou, X., Zhang, W., Xiong, W., Wang, L., Zhang, S., Wang, P., & Wang, C. (2018). Integration of life cycle assessment and statistical analysis to understand the influence of rainfall on WWTPs with combined sewer systems. *Journal of Cleaner Production, 172*, 2521-2530. https://doi.org/10.1016/j.jclepro.2017.11.158

Liehr, G. A., Zettler, M. L., Leipe, T., & Witt, G. (2005). The ocean quahog arctica islandica L.: A bioindicator for contaminated sediments. *Marine Biology, 147*(3), 671-679. https://doi.org/10.1007/s00227-005-1612-y

Liu, M., Gonzalez, J. E., Willis, L. B., & Walker, G. C. (1998). A novel screening method for isolating exopolysaccharide-deficient mutants. *Applied and Environmental Microbiology, 64*(11), 4600-4602. https://doi.org/10.1128/aem.64.11.4600-4602.1998

Liu, Y., & Chen, J. (2008). Phosphorus cycle. In S. E. Jørgensen, & B. D. Fath (Eds.), *Encyclopedia of ecology* (pp. 2715-2724). Academic Press. https://doi.org/10.1016/B978-008045405-4.00754-0

Mahaut, V., & Andrieu, H. (2019). Relative influence of urban-development strategies and water management on mixed (separated and combined) sewer overflows in the context of climate change and population growth: A case study in nantes. *Sustainable Cities and Society, 44*, 171-182. https://doi.org/10.1016/j.scs.2018.09.012

Masanja, F., Yang, K., Xu, Y., He, G., Liu, X., Xu, X., Jiang, X., Luo, X., Mkuye, R., Deng, Y., & Zhao, L. (2023). Bivalves and microbes: A mini-review of their relationship and potential implications for human health in a rapidly warming ocean. *Frontiers in Marine Science, 10*https://doi.org/10.3389/fmars.2023.1182438

Meiklejohn, J. (1952). Minimum phosphate and magnesium requirements of nitrifying bacteria. *Nature (London), 170*(4339), 1131. https://doi.org/10.1038/1701131a0

Milan, M., Carraro, L., Fariselli, P., Martino, M. E., Cavalieri, D., Vitali, F., Boffo, L., Patarnello, T., Bargelloni, L., & Cardazzo, B. (2018). Microbiota and environmental stress: How pollution affects microbial communities in manila clams. *Aquatic Toxicology, 194*, 195-207. https://doi.org/10.1016/j.aquatox.2017.11.019

Mitraka, G., Kontogiannopoulos, K. N., Batsioula, M., Banias, G. F., Zouboulis, A. I., & Kougias, P. G. (2022). A comprehensive review on pretreatment methods for enhanced biogas production from sewage sludge. *Energies (Basel), 15*(18), 6536. https://doi.org/10.3390/en15186536

Monds, R. D., Newell, P. D., Schwartzman, J. A., & O'Toole, G. A. (2006). Conservation of the pho regulon in *Pseudomonas fluorescens* Pf0-1. *Applied and Environmental Microbiology, 72*(3), 1910-1924. https://doi.org/10.1128/AEM.72.3.1910-1924.2006

Morlino, M. S., Serna García, R., Savio, F., Zampieri, G., Morosinotto, T., Treu, L., & Campanaro, S. (2023). *Cupriavidus necator* as a platform for polyhydroxyalkanoate production: An overview of strains, metabolism, and modeling approaches. *Biotechnology Advances, 69*, 108264. https://doi.org/10.1016/j.biotechadv.2023.108264

Murphy, J., & Riley, J. P. (1962). A modified single solution method for the determination of phosphate in natural waters. *Analytica Chimica Acta, 27*, 31-36. https://doi.org/10.1016/S0003-2670(00)88444-5

Nabaterega, R., Kumar, V., Khoei, S., & Eskicioglu, C. (2021). A review on two-stage anaerobic digestion options for optimizing municipal wastewater sludge treatment process. *Journal of Environmental Chemical Engineering, 9*(4), 105502. https://doi.org/10.1016/j.jece.2021.105502

Narayanan, M., Kandasamy, S., Kumarasamy, S., Gnanavel, K., Ranganathan, M., & Kandasamy, G. (2020). Screening of polyhydroxybutyrate producing indigenous bacteria from polluted lake soil. *Heliyon, 6*(10), e05381. https://doi.org/10.1016/j.heliyon.2020.e05381

Nedelciu, C. E., Ragnarsdottir, K. V., Schlyter, P., & Stjernquist, I. (2020). Global phosphorus supply chain dynamics: Assessing regional impact to 2050. *Global Food Security, 26*, 100426. https://doi.org/10.1016/j.gfs.2020.100426

Nguyen, P. Y., Marques, R., Wang, H., Reis, M. A. M., Carvalho, G., & Oehmen, A. (2023). The impact of pH on the anaerobic and aerobic metabolism of tetrasphaera-enriched polyphosphate accumulating organisms. *Water Research X, 19*, 100177. https://doi.org/10.1016/j.wroa.2023.100177

Ni, M., Pan, Y., Zhang, X., Wen, L., Yang, W., Chen, Y., Huang, Y., & Song, Z. (2021). Effects of P/C ratios on the growth, phosphorus removal and phosphorus recovery of a novel strain of highly efficient PAO. *Process Biochemistry (1991), 111*(1), 109-117. https://doi.org/10.1016/j.procbio.2021.08.010

Norðurorka. (n.d.a). *Fráveitan í tölum.* nordurorka.is. Retrieved January 25, 2024, from https://www.no.is/is/veiturnar-okkar/fraveita/hreinsistod-fraveitu

Norðurorka. (n.d.b). *Kortasjá norðurorku.* no.is. Retrieved 29/03/2024, from https://map.is/no/@539853,576307,z3.4685733063161592,1

Norðurorka. (2023). [Results from sewage sampling in 2022 and 2023 at the wastewater treatment plant in Akureyri].

Novák, L., Zubáčová, Z., Karnkowska, A., Kolisko, M., Hroudová, M., Stairs, C. W., Simpson, A. G. B., Keeling, P. J., Roger, A. J., Čepička, I., & Hampl, V. (2016). Arginine deiminase pathway enzymes: Evolutionary history in metamonads and other eukaryotes. *BMC Evolutionary Biology, 16*(1), 197. https://doi.org/10.1186/s12862-016-0771-4

OECD. (2001). Test no. 303: Simulation test - aerobic sewage treatment -- A: Activated sludge units; B: Biofilms. *OECD guidelines for the testing of chemicals, section 3 degradation and accumulation* (). OECD Publishing. https://doi.org/10.1787/9789264070424-en

Onnis-Hayden, A., Srinivasan, V., Tooker, N. B., Li, G., Wang, D., Barnard, J. L., Bott, C., Dombrowski, P., Schauer, P., Menniti, A., Shaw, A., Stinson, B., Stevens, G., Dunlap, P., Takács, I., McQuarrie, J., Phillips, H., Lambrecht, A., Analla, H., . . . Gu, A. Z. (2019). Survey of full-scale sidestream enhanced biological phosphorus removal (S2EBPR) systems and comparison with conventional EBPRs in north america: Process stability, kinetics, and microbial populations. *Water Environment Research, 92*(3), 403-417. https://doi.org/10.1002/wer.1198

Paytan, A., & McLaughlin, K. (2007). The oceanic phosphorus cycle. *Chemical Reviews, 107*(2), 563-576. https://doi.org/10.1021/cr0503613

Peacock, M. (2021). Phosphate metabolism in health and disease. *Calcified Tissue International, 108*(1), 3-15. https://doi.org/10.1007/s00223-020-00686-3

Pei, P., Aslam, M., Wang, H., Ye, P., Li, T., Liang, H., Lin, Q., Chen, W., & Du, H. (2024). Diversity and ecological function of urease-producing bacteria in the cultivation environment of gracilariopsis lemaneiformis. *Microbial Ecology, 87*(1), 35. https://doi.org/10.1007/s00248-023-02339-y

Pinhal, S., Ropers, D., Geiselmann, J., & de Jong, H. (2019). Acetate metabolism and the inhibition of bacterial growth by acetate. *Journal of Bacteriology, 201*(13), 147. https://doi.org/10.1128/JB.00147-19

Porras, M. A., Villar, M. A., & Cubitto, M. A. (2017). Novel spectrophotometric technique for rapid determination of extractable PHA using sudan black dye. *Journal of Biotechnology, 255*, 28-32. https://doi.org/10.1016/j.jbiotec.2017.06.012

Preisner, M., Neverova-Dziopak, E., & Kowalewski, Z. (2020). Analysis of eutrophication potential of municipal wastewater. *Water Science and Technology, 81*(9), 1994-2003. https://doi.org/10.2166/wst.2020.254

Qadir, M., Drechsel, P., Jiménez Cisneros, B., Kim, Y., Pramanik, A., Mehta, P., & Olaniyan, O. (2020). Global and regional potential of wastewater as a water, nutrient and energy source. *Natural Resources Forum, 44*(1), 40-51. https://doi.org/10.1111/1477-8947.12187

Reglugerð um fráveitur og skólp nr. 798, (1999). https://island.is/reglugerdir/nr/0798-1999

Rorat, A., Courtois, P., Vandenbulcke, F., & Lemiere, S. (2019). Sanitary and environmental aspects of sewage sludge management. *Industrial and municipal sludge* (pp. 155-180). Elsevier. https://doi.org/10.1016/b978-0-12-815907-1.00008-8

Sallam, K. I. (2007). Antimicrobial and antioxidant effects of sodium acetate, sodium lactate, and sodium citrate in refrigerated sliced salmon. *Food Control, 18*(5), 566-575. https://doi.org/10.1016/j.foodcont.2006.02.002

Samorka og Samband íslenskra sveitarfélaga. (2020). *Minnisblað: Álit samtakanna vegna tillagna um aukna eins þreps hreinsun skólpsí drögum að nýrri reglugerð um fráveitur og skólp.* Samorka. https://samorka.is/wp-content/uploads/2021/10/Minnisblad-um-tillogur-um-aukna-fraveituhreinsun-061120.pdf

Samuel, L. P., Balada-Llasat, J., Harrington, A., & Cavagnolo, R. (2016). Multicenter assessment of gram stain error rates. *Journal of Clinical Microbiology, 54*(6), 1442-1447. https://doi.org/10.1128/JCM.03066-15

Santos-Beneit, F. (2015). The pho regulon: A huge regulatory network in bacteria. *Frontiers in Microbiology, 6*, 402. https://doi.org/10.3389/fmicb.2015.00402

Saranya, K., Sundaramanickam, A., Manupoori, S., & Kanth, S. V. (2022). Screening of multi-faceted phosphate-solubilising bacterium from seagrass meadow and their plant growth promotion under saline stress condition. *Microbiological Research, 261*, 127080. https://doi.org/10.1016/j.micres.2022.127080

Sathya, A. B., Sivasubramanian, V., Santhiagu, A., Sebastian, C., & Sivashankar, R. (2018). Production of polyhydroxyalkanoates from renewable sources using bacteria. *Journal of Polymers and the Environment, 26*(9), 3995-4012. https://doi.org/10.1007/s10924-018-1259-7

Schone, B. (2013). Arctica islandica (bivalvia): A unique paleoenvironmental archive of the northern north atlantic ocean. *Global and Planetary Change, 111*, 199-225. https://doi.org/10.1016/j.gloplacha.2013.09.013

Serafim, L. S., Lemos, P. C., Levantesi, C., Tandoi, V., Santos, H., & Reis, M. A. (2002). Methods for detection and visualization of intracellular polymers stored by polyphosphate-accumulating micro-organisms. *Journal of Microbiological Methods, 51*(1), 1-18. https://doi.org/https://doi.org/10.1016/S0167-7012(02)00056-8

Smol, M., Preisner, M., Bianchini, A., Rossi, J., Hermann, L., Schaaf, T., Kruopienė, J., Pamakštys, K., Klavins, M., Ozola-Davidane, R., Kalnina, D., Strade, E., Voronova, V., Pachel, K., Yang, X., Steenari, B., & Svanström, M. (2020). Strategies for sustainable and circular management of phosphorus in the baltic sea region: The holistic approach of the InPhos project. *Sustainability (Basel, Switzerland), 12*(6), 2567. https://doi.org/10.3390/su12062567

Strahl, J., & Abele, D. (2020). Nitric oxide mediates metabolic functions in the bivalve *Arctica islandica* under hypoxia. *PloS One, 15*(5), e0232360. https://doi.org/10.1371/journal.pone.0232360

Tarayre, C., Nguyen, H., Brognaux, A., Delepierre, A., De Clercq, L., Charlier, R., Michels, E., Meers, E., & Delvigne, F. (2016). Characterisation of phosphate accumulating organisms and techniques for polyphosphate detection: A review. *Sensors, 16*(6), 797-14. https://doi.org/10.3390/s16060797

Thakur, I. S., & Medhi, K. (2019). Nitrification and denitrification processes for mitigation of nitrous oxide from waste water treatment plants for biovalorization: Challenges and opportunities. *Bioresource Technology, 282*, 502-513. https://doi.org/10.1016/j.biortech.2019.03.069

The jamovi project. (2021). *Jamovi. (Version 2.2) [Computer software]. https://www.jamovi.org*

Thorndahl, S., Balling, J. D., & Larsen, U. B. B. (2016). Analysis and integrated modelling of groundwater infiltration to sewer networks. *Hydrological Processes, 30*(18), 3228-3238. https://doi.org/10.1002/hyp.10847

Tindall, B. J., Sikorski, J., Smibert, R. A., & Krieg, N. R. (2007). Phenotypic characterization and the principles of comparative systematics. *Methods for general and molecular microbiology* (3rd Edition, pp. 330-393). ASM Press. https://doi.org/10.1128/9781555817497.ch15

Umhverfisstofnun. (2023). *Stöðuskýrsla fráveitumála 2022.* Umhverfisstofnun. http://co2.ust.is/haf-og-vatn/fraveitumal/stada-fraveitumala/

United nations. (n.d.). *The 17 goals.* Retrieved 22 Apr, 2024, from https://sdgs.un.org/goals

Valtýsson, H. Þ, & Jónsson, S. (2000). Sjór og sjávarlíf. In B. Guðmundsson (Ed.), *Líf í eyjafirði* (pp. 123-164). Rannsóknastofnun Háskólans á Akureyri.

Verma, A., Wei, X., & Kusiak, A. (2013). Predicting the total suspended solids in wastewater: A data-mining approach. *Engineering Applications of Artificial Intelligence, 26*(4), 1366-1372. https://doi.org/10.1016/j.engappai.2012.08.015

Vicente, D., Proença, D. N., & Morais, P. V. (2023). The role of bacterial polyhydroalkanoate (PHA) in a sustainable future: A review on the biological diversity. *International Journal of Environmental Research and Public Health, 20*(4), 2959. https://doi.org/10.3390/ijerph20042959

Vrede, K., Heldal, M., Norland, S., & Bratbak, G. (2002). Elemental composition (C, N, P) and cell volume of exponentially growing and nutrient-limited bacterioplankton. *Applied and Environmental Microbiology, 68*(6), 2965-2971. https://doi.org/10.1128/AEM.68.6.2794-2801.2002

Watcharawipas, A., Watanabe, D., & Takagi, H. (2018). Sodium acetate responses in *Saccharomyces cerevisiae* and the ubiquitin ligase Rsp5. *Frontiers in Microbiology, 9*, 2495. https://doi.org/10.3389/fmicb.2018.02495

Wen, Q., Chen, Z., Tian, T., & Chen, W. (2010). Effects of phosphorus and nitrogen limitation on PHA production in activated sludge. *Journal of Environmental Sciences (China), 22*(10), 1602-1607. https://doi.org/10.1016/S1001-0742(09)60295-3

Woodard & Curran Inc. (2006). 5 - waste characterization. *Industrial waste treatment handbook* (2. ed., pp. 83-126). Elsevier. https://doi.org/10.1016/B978-0-7506-7963-3.X5000-0

Xie, X., Deng, X., Chen, L., Yuan, J., Chen, H., Wei, C., Liu, X., Wuertz, S., & Qiu, G. (2024). Integrated genomics provides insights into the evolution of the polyphosphate accumulation trait of *Ca.* Accumulibacter. *Environmental Science and Ecotechnology, 20*, 100353. https://doi.org/10.1016/j.ese.2023.100353

Yuan, Z., Jiang, S., Sheng, H., Liu, X., Hua, H., Liu, X., & Zhang, Y. (2018). Human perturbation of the global phosphorus cycle: Changes and consequences. *Environmental Science & Technology, 52*(5), 2438-2450. https://doi.org/10.1021/acs.est.7b03910

Yuan, Feng, Yin, S., Xu, Y., Xiang, L., Wang, H., Li, Z., Fan, K., & Pan, G. (2021). The richness and diversity of catalases in bacteria. *Frontiers in Microbiology, 12*, 645477. https://doi.org/10.3389/fmicb.2021.645477

Zagklis, D. P., & Bampos, G. (2022). Tertiary wastewater treatment technologies: A review of technical, economic, and life cycle aspects. *Processes, 10*(11), 2304. https://doi.org/10.3390/pr10112304

Zhang, C., Guisasola, A., & Baeza, J. A. (2022). A review on the integration of mainstream P-recovery strategies with enhanced biological phosphorus removal. *Water Research (Oxford), 212*, 118102. https://doi.org/10.1016/j.watres.2022.118102

Zhang, Y., Qiu, X., Luo, J., Li, H., How, S., Wu, D., He, J., Cheng, Z., Gao, Y., & Lu, H. (2024). A review of the phosphorus removal of polyphosphate-accumulating organisms in natural and engineered systems. *The Science of the Total Environment, 912*, 169103. https://doi.org/10.1016/j.scitotenv.2023.169103

Zhao, H., Ma, Y., Fang, J., Hu, L., & Li, X. (2022). Particle size distribution and total suspended solid concentrations in urban surface runoff. *The Science of the Total Environment, 815*, 152533. https://doi.org/10.1016/j.scitotenv.2021.152533

Zhao, L., Ni, Y., Su, M., Li, H., Dong, F., Chen, W., Wei, R., Zhang, L., Guiraud, S. P., Martin, F., Rajani, C., Xie, G., & Jia, W. (2017). High throughput and quantitative measurement of microbial metabolome by gas chromatography/mass spectrometry using automated alkyl

chloroformate derivatization. *Analytical Chemistry (Washington), 89*(10), 5565-5577. https://doi.org/10.1021/acs.analchem.7b00660

Zhao, M., Xu, Y., Zhang, C., Rong, H., & Zeng, G. (2016). New trends in removing heavy metals from wastewater. *Applied Microbiology and Biotechnology, 100*(15), 6509-6518. https://doi.org/10.1007/s00253-016-7646-x

Zimbro, M. J., Power, D. A., Miller, S., M., Wilson, G. E., & Johnson, J. A. (2009). *Difco & BBL manual*. Becton, Dickinson and Company.

Appendices

Appendix 1 - List of media compositions

Basal mineral medium composition can be seen in Table 7.

Table 7: Composition of basal mineral medium.

Substance	Amount (g/L)
Sodium phosphate monobasic dihydrate	3.04
Sodium phosphate dibasic dihydrate	5.43
Sodium chloride	0.3
Calcium chloride dihydrate	0.11
Magnesium dichloride hexahydrate	0.1
Sodium bicarbonate	0.8
Yeast extract	2.0
Resazurin	0.001

National Botanical Research Institute's phosphate (NBRIP) growth medium composition can be seen in Table 8.

Table 8: Composition of NBRIP growth medium.

Substance	Amount (g/L)
Agar	15
Glucose	10
Calcium phosphate	5
Magnesium chloride hexahydrate	5
Magnesium sulphate heptahydrate	0.25
Potassium chloride	0.2
Ammonium sulphate	0.1

Moller‘s broth base composition can be seen in Table 9.

Table 9: Composition of Moller's broth base.

Substance	Amount
Difco Proteose Peptone 3 or Thiotone BBL	5.0 g
Beef extract	5.0 g
Glucose	0.5 g
Bromocresol purple solution	625 µL
0.2% cresol red solution	5 mg
Pyridoxal	5 mg
Distilled water	1 L

The composition of OECD SWW can be seen in Table 10.

Table 10: Composition of OECD SWW. The amount of phosphate and acetate sources varied between the P1-3 and A1-3 conditions, as represented by numbers from 1 to 3.

Substance	Amount (mg/L)		
Peptone	160		
Meat extract	110		
Urea	30		
Sodium chloride (Honeywell, ref. 31434)	7		
Calcium chloride dihydrate	4		
Magnesium sulphate heptahydrate	2		
	1	2	3
Anhydrous dipotassium hydrogen phosphate	28	56	140
Sodium acetate	0	120	240

The C/P ratios of all the different phosphate and acetate OECD SWW conditions can be seen in Table 11.

Table 11: The C/P ratios of the different phosphate and acetate conditions in the OECD SWW.

SWW condition	C/P ratio
P1A1	0
P1A2	6.6
P1A3	13.1
P2A1	0.0
P2A2	3.2
P2A3	6.4
P3A1	0.0
P3A2	1.3
P3A3	2.6

The composition of Syntho SWW can be seen in Table 12.

Table 12: Composition of Syntho SWW. The amount of phosphate and acetate sources varied between the P1-4 and A1-4 conditions, as represented by numbers from 1 to 4.

Substance	Amount (mg/L)			
Peptone	15			
Meat extract	15			
Glycerol 85%	40			
Starch	50			
Skim milk powder	120			
Urea	75			
Ammonium chloride	11			
Uric acid	9			
SDS	10			
Calcium dichloride	5			
Sodium bicarbonate	25			
Iron(II) sulphate heptahydrate	10			
Diatomaceous earth	10			
	1	2	3	4
Disodium hydrogen phosphate dihydrate (Na_2HPO_4 * 2 H_2O)	13	25	125	250
Potassium phosphate tribasic (K_3PO_4)	10	20	100	200
Sodium acetate	0	120	1200	12000

The C/P ratios of all the different phosphate and acetate Syntho SWW conditions can be seen in Table 13.

Table 13: The C/P ratios of the different phosphate and acetate conditions in the Syntho SWW.

SWW condition	C/P ratio
P1A1	0.0
P1A2	12.5
P1A3	124.7
P1A4	1247.2
P2A1	0.0
P2A2	6.2
P2A3	62.4
P2A4	623.6
P3A1	0.0
P3A2	1.2
P3A3	12.5
P3A4	124.7
P4A1	0.0
P4A2	0.6
P4A3	6.2
P4A4	62.4

Appendix 2 - Experimental results

A list of reactivated strains, their media of isolation and morphology notes can be seen in Table 14.

Table 14: All reactivated strains, their media of isolation and morphology notes.

Strain	Media	Morphology notes
CL131	MA	Milky, lobate, smooth
CL188	MA	Orange, lobate, dry
CL197	PCA	Milky, round, smooth
CL198	PCA	Milky, round smooth
CL209	NA	Yellowish, round, smooth, slimy
CL214	NA	Milky, round, smooth
CL217	NA	Milky, round, smooth
CL218	NA	Milky, round, smooth, small colonies
CL226	NA	Milky, round, smooth, small colonies
CL227	NA	Yellowish, round, smooth, small colonies
CL230	NA	Yellowish, round
CL235	NA	Orange, irregular
CL239	MA	Orange, round, smooth, slimy
CL240	MA	Yellowish, round, smooth
CL241	MA	Milky, lobate, smooth
CL242	MA	Milky, round, smooth, slimy
CL245	NA	Milky, lobate, smooth, small colonies
CL247	MA	Orangish, lobate, smooth
CL259	MA	Yellowish, lobate, smooth
CL260	MA	Orange, round, smooth, syrup-like texture
CL261	MA	Orange, round, smooth, small colonies

CL262	MA	Orangish, round, smooth
CL266	MA	Orange, round, smooth
CL267	MA	Dark-orange, round, smooth, slimy
CL273	MA	Yellowish, lobate, smooth
CL274	MA	Yellowish, lobate, smooth
CL275	MA	Milky, round, smooth, slimy
CL276	MA	Orangish, round, smooth
CL277	MA	Orange, round, smooth, slimy
CL278	MA	Orange, round, smooth, syrup-like texture
CL279	MA	Milky, lobate, smooth
CL280	MA	Milky, lobate, smooth
CL281	MA	Milky, lobate, smooth

Phosphate mobilization results for reactivated strains, excluding the five strains that were chosen for continued work (CL131, CL188, CL197, CL198 and CL242) can be seen in Table 15.

Table 15: Phosphate mobilization results for all reactivated strains, excluding the five selected ones (CL131, CL188, CL197, CL198 and CL242). Strains which were streaked on NBRIP+NaCl were also streaked on MAP. No halo formation is represented by -, halo formation is represented by +.

Media	NBRIP	NBRIP+NaCl	MAP
CL214	+	N/A	N/A
CL217	+	N/A	N/A
CL218	+	N/A	N/A
CL226	+	N/A	N/A
CL227	+	N/A	N/A
CL235	+	N/A	N/A
CL239	N/A	-	-
CL240	N/A	+	-

CL241	N/A	+	-
CL245	+	N/A	N/A
CL247	N/A	+	-
CL259	N/A	-	-
CL260	N/A	-	-
CL261	N/A	-	-
CL262	N/A	+	-
CL266	N/A	-	-
CL273	N/A	+	-
CL274	N/A	+	-
CL275	N/A	+	-
CL276	N/A	+	-
CL278	N/A	-	-
CL279	N/A	-	-
CL280	N/A	+	-
CL281	N/A	+	-

Appendix 3 - PCR and electrophoresis results

The 16S PCR program specifications are shown in Table 16.

Table 16: 16S PCR program specifications. The white area represents different periods of the same cycle, which was repeated 35 times. The grey areas represent a single cycle.

Temperature	Duration	Repetitions
95°C	30 sec	1x
95°C	30 sec	
58°C	30 sec	35x
68°C	90 sec	
68°C	5 mins	1x
4°C	Forever	1x

The gel on which the band from the CL131 PCR product was visualized can be seen in Figure 21. A 100 bp ladder was used, the band of CL131 is close to the 1500 bp reference band, indicating that the PCR product is approximately 1500 bp long.

Figure 21: Band of CL131 visualized on gel after PCR and electrophoresis. The band is just below the 1500 bp reference band on the 100 bp ladder.

The gel on which the bands from the CL197 and CL242 PCR products were visualized can be seen in Figure 22. The vague band in well 4 is from CL197, while the band in well 15 is from CL242. A 1 kb ladder was used, the bands of CL242 and CL197 are close to the 1500 bp reference band, indicating that the PCR product is approximately 1500 bp long. The specimens put in wells 6-9 contained bacterial colonies which were put straight into the mastermix, without DNA extraction.

Figure 22: Bands of CL242 (well 15) and CL197 (well 4) visualized on gel after PCR and electrophoresis. The bands are just below the 1500 bp reference band on the 1 kb ladder.